Chemical Effects during Modification of Kraft Lignin with Ozone under Alkaline Conditions

OLIVER MUSL

DIPLOMA THESIS

supervised by

**Univ.Prof. Dipl.-Chem. Dr.rer.nat. Dr.h.c.
Thomas Rosenau
Univ.-Ass. Dipl.-Ing. Dr. Stefan Böhmdorfer**

realized at the
Department für Chemie
Abteilung für Chemie nachwachsender Rohstoffe
Universität für Bodenkultur Wien

submitted at the

Universität für Bodenkultur

University of Natural Resources and Life Sciences

Vienna, Austria

Vienna, September 2017

Affidavit

I hereby declare that I am the sole author of this work. No assistance other than that which is permitted has been used. Ideas and quotes taken directly or indirectly from other sources are identified as such. This written work has not yet been submitted in any part.

Eidesstaatliche Erklärung

Ich erkläre eidesstattlich, dass ich die Arbeit selbständig angefertigt habe. Es wurden keine anderen als die angegebenen Hilfsmittel benutzt. Die aus fremden Quellen direkt oder indirekt übernommenen Formulierungen und Gedanken sind als solche kenntlich gemacht. Diese schriftliche Arbeit wurde noch an keiner Stelle vorgelegt.

Date: _____   Signature: _____

Acknowledgement

At this point, I would like to thank all those people who have been a great source of help to me and without whom I would not have been able to accomplish my diploma thesis, at least not in its present form. Beside the indeed supreme assistance in scientific matters that I was able to enjoy, I also would like to thank all those who provided me the emotional support during this challenging and tedious time, which granted me enough perserverance to attain my goals at last.

Primarily, I would like to thank all the members of the Division of Chemistry of Renewable Resources, for their warm and friendly affiliation to the group and their kind support and guidance in all situations during my work in the lab. You made this thesis a wonderful experience for me and I am really looking forward to work with the team again soon. Apart from that, I would like to express my sincere thanks to a few people whose contributions were essential for the accomplishment of this thesis.

With regard to this work, I would like to express my utmost gratitude to…

… **Dipl.-Ing. Dr. Stefan Böhmdorfer**, Division of Chemistry of Renewable Resources, for his indispensable guidance and support as well as for being an excellent mentor and motivator throughout the whole thesis. His positive encouragement gave me finally the necessary confidence in my abilities, exciting me to tackle my tasks with the greatest ambition and devotion. The opportunity to work under his supervision and direction was definitely a very pleasant and delightful matter, that I would not want to miss.

… **Dipl.-Ing. Dr. Sonja Schiehser**, Division of Chemistry of Renewable Resources, for being my key ally in the difficult and troublesome task of GC-MS. This thesis would have been quite a lot shorter, if it was not for her engagement and her incredible experience.

… **Stefan Winklehner Bsc.**, friend and fellow student, for his help in all respects in the lab and for his useful practical tricks, helping me to save lots of worthwile time while avoiding frustrating failures due to ignorance.

… **Dr. Ivan Sumerskii**, Division of Chemistry of Renewable Resources, for his proficient advice throughout my work in the lab and especially during the performance of his fractionation method, the resin assisted extraction.

… **Ing. Marion Sumetzberger-Hasinger**, Institute of Environmental Biotechnology (IFA Tulln) of Boku University, for carrying out the NPOC measurements for me. Not only sparing me a lot of time, but also providing me with a load of important data.

Abstract

The aim of this study was to investigate the chemical effects during the modification of Kraft lignin with ozone under alkaline conditions. Primarily, the influence of alkalinity on the modification process was studied, therefore three experiments varying in initial pH were carried out. The change to the lignin was monitored over time by the analyses of dry matter, non-purgeable organic carbon and UV-Vis measurements. Further information on the chemical composition of the modified samples were gained from an applied fractionation, including acidic precipitation and resin assisted extraction. In addition, identification and quantification of small carboxylic and hydroxylated degradation products were performed by GC-MS. Initial pH was found to be crucial to the degree of volatilization as well as to the solubilization of aromatic moieties. GC-MS quantification showed a distinct predominance of oxalic acid, followed by glycolic and tartronic acid. Clustering of the GC-MS results according to the degradation model by KUITUNEN ET AL. (2011) indicated a predominance of ring-opening reactions over side chain cleavage in the modification process. However, the applicability of the degradation model on lignin modification with ozone was found to be limited as the degree of volatilization was heavily underestimated.

Keywords: lignin, ozone, modification, oxidation, alkaline, GC-MS

Kurzzusammenfassung

Das Ziel dieser Arbeit bestand darin, die chemischen Auswirkungen auf Kraft Lignin durch die Modifizierung mit Ozon unter basischen Bedingungen zu untersuchen. Zu diesem Zweck wurden drei Lignin-Lösungen mit Ozon versetzt, die sich in ihrem ursprünglichen pH-Wert unterschieden. Die Veränderungen am Lignin wurden mittels Trockenmassebestimmung, Bestimmung des nicht ausblasbaren organischen Kohlenstoffs und UV-Vis-Spektroskopie charakterisiert. Eine Fraktionierung der modifizierten Proben durch saure Fällung und selektive Extraktion brachte zusätzliche Informationen zu deren chemischer Zusammensetzung. Durch die Anwendung von GC-MS konnten mehrere nicht flüchtige Abbauprodukte in den modifizierten Proben identifiziert und quantifiziert werden. Es konnte festgestellt werden, dass der ursprüngliche pH-Wert der Lignin-Lösungen einen entscheidenden Einfluss sowohl auf die Entstehung volatiler Abbauprodukte hat, als auch auf die Solubilisierung von aromatischen Komponenten. Die Quantifizierung von Abbauprodukten durch GC-MS zeigte, dass primär Oxalsäure gefolgt von Glycol- und Tartronsäure im Laufe des Prozesses gebildet wird. Die Gruppierung der GC-MS Ergebnisse gemäß des Modells von KUITUNEN ET AL. (2011) ergab, dass während der Modifikation Ringöffnungsreaktionen wesentlich häufiger auftreten als die Abspaltung von Seitenketten. Allerdings stellte sich das Modell für die Beschreibung von Ligninmodifikation mit Ozon als nur begrenzt anwendbar dar, da die Entstehung von volatilen Abbauprodukten durch das Modell stark unterschätzt wurde.

Schlagwörter: Lignin, Ozon, Modifizierung, Oxidation, alkalisch, GC-MS

Contents

List of Abbreviations

BSTFA	N,O-bis(trimethylsilyl)-triflouroacetamide
Ca^{2+}	calcium ion
^{13}C-GCP	^{13}C labeled glucose conversion product
COD	chemical oxygen demand
CO_2	carbon dioxide
DMAP	4-(dimethylamino)-pyridine
DMS	dimethyl sulfide
GC	gas chromatography
HCl	hydrogen chloride
LCC	lignin-carbohydrate complexes
MGP	methyl-α-D-galactopyranoside
MS	mass spectroscopy
Na^+	sodium ion
$NaBH_4$	sodium borohydride
NaH_2PO_4	sodium dihydrogen phosphate
Na_2HPO_4	disodium hydrogen phosphate
NaOH	sodium hydroxide
Na_2S	sodium sulfide
NH_4^+	ammonium ion
NPOC	non-purgeable organic carbon
SHE	standard hydrogen electrode
TOC	total organic carbon
TMCS	chlorotrimethylsilane
UV	ultraviolet
UV-Vis	ultraviolet–visible
VPSA	vacuum pressure swing adsorption

1 Introduction

1.1 Lignin

Lignin is one of the main constituents of all dry-land plant cell wall. It is the second most abundant biopolymer in the world right after cellulose. Its widespread appearance in the realm of plants is not only due to its ability of imparting rigidity to the cell walls, enabling the growth of huge structures as trees, but also for its use in facilitating an internal transport system of water, nutrients and metabolites, and since it causes effective resistance against microbial decay (SARKANEN & LUDWIG, 1971A).
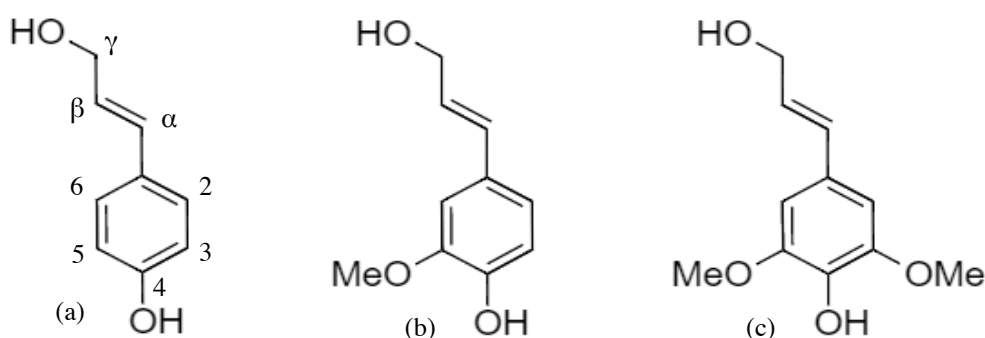

Figure 1: Chemical Formula, and atom numbering for the three main lignin monomers: (a) *p*-coumaryl alcohol, (b) coniferyl alcohol, (c) sinapyl alcohol (CALVO-FLORES, DOBADO, ISAC-GARCIA, & MARTIN-MARTINEZ, 2015).

In contrast to the linear cellulose polymer chains, lignin is a structurally rather heterogenous and spatially complex polymer, showing quite different physical and chemical properties depending on its natural origin (CALVO-FLORES ET AL., 2015). Its unique structural diversity derives simply from the manifold combination of three phenylpropane derivatives, so-called monolignols (Figure 1) by enzyme-initiated dehydrogenative polymerization in its biosynthesis (CALVO-FLORES ET AL., 2015; DIMMEL, 2010; RALPH ET AL., 2004; SARKANEN & LUDWIG, 1971A). In this oxidative mechanism, coupling occurs mainly between phenolic radicals of the monomers with phenoxy radicals within the macromolecule, which are exhibiting an unpaired electron density delocalized over various positions (Figure 2), allowing a number of possible linkages and therefore resulting in the complex and unordered polymer. Overall, the C-β position appears to be the most reactive one, and is involved in the majority of linkages (up to 75%), including the most predominant β-aryl ether linkage (Figure 3) (BRUNOW & LUNDQUIST, 2010; RALPH ET AL., 2004). Although they occur less frequently in lignin, covalent C – C linkages (Figure 3), referred to as condensed structures, are particularly of interest, as they show much higher stability than the C – O ether linkages (DIMMEL, 2010; RALPH ET AL., 2004). Additionally, a methoxy group present at C-3 (coniferyl alcohol) and C-5 (sinapyl alcohol) will prevent linkages at these positions, thus leading to lignins with different properties, depending on their composition of monolignols (RALPH ET AL., 2004).
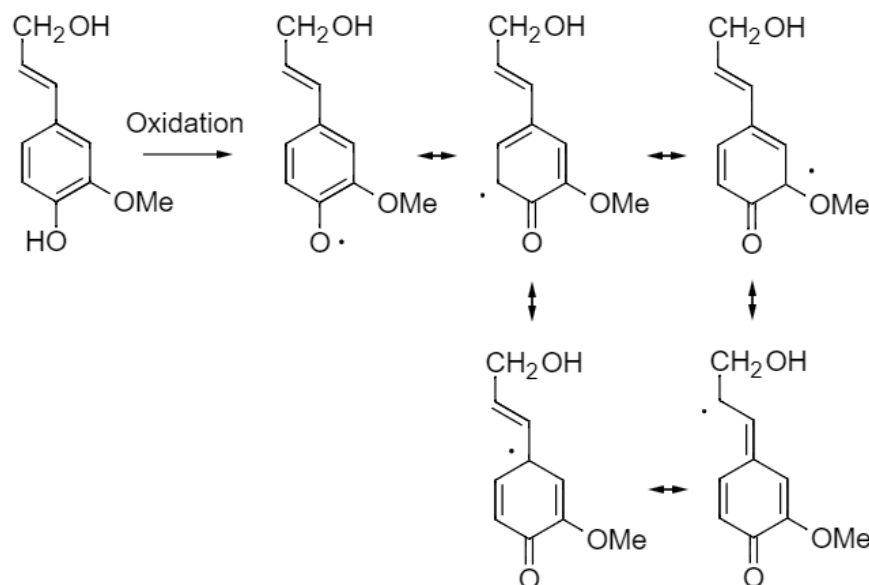
Figure 2: Resonance Lewis structures for the coniferyl alcohol radical (DIMMEL, 2010).

This is also the very reason for the substantial difference observed between gymnosperm (softwood) and angiosperm (hardwood) lignins in terms of physical and chemical properties. More precisely, softwood lignins are almost exclusively based on guaiacyl units deriving from coniferyl alcohol, whereas hardwood lignins consist of a mixture of guaiacyl and syringyl units, which are derived from sinapyl alcohol (SARKANEN & HERGERT, 1971). Consequently, the content of methoxy groups is higher on average in hardwood lignins, leading to less condensed structures and therefore to a much higher reactivity in general (BRUNOW & LUNDQUIST, 2010). Moreover, branching occurs in softwood lignins largely through dibenzodioxocin and biphenyl ether linkages (Figure 3) resulting in rather compact structures, while hardwood lignins appear to be more linear in dependence to their G/S ratio (guaiacyl to syringyl units), as the additional methoxy group in syringyl units hinders the formation of linkages at the C-5 position (RALPH ET AL., 2004).

These differences in shape and reactivity can also be expressed by the means of linkage distribution, in which softwood lignins exhibit lower amounts of β-aryl ether units (35%), but higher amounts of biphenyl units (23%), which are partly present as dibenzodioxocin (6%) units, compared to hardwood lignins. In contrast, these show a predominant amount of β-aryl ether units (45%) and only a small amount of biphenyl units (9%), which are hardly present as dibenzodioxocin (1%). Minor differences between softwood and hardwood lignins can be observed in the amounts of phenylcoumaran (10 vs. 4%), pinoresinol (4 vs. 8%) and biphenyl ether units (4 vs. 7%) (Figure 3) (BRUNOW & LUNDQUIST, 2010). In Figure 4, models of isolated lignins are shown, depicting the structural differences between softwood and hardwood lignins in terms of average linkage distribution and ratio of monolignols.
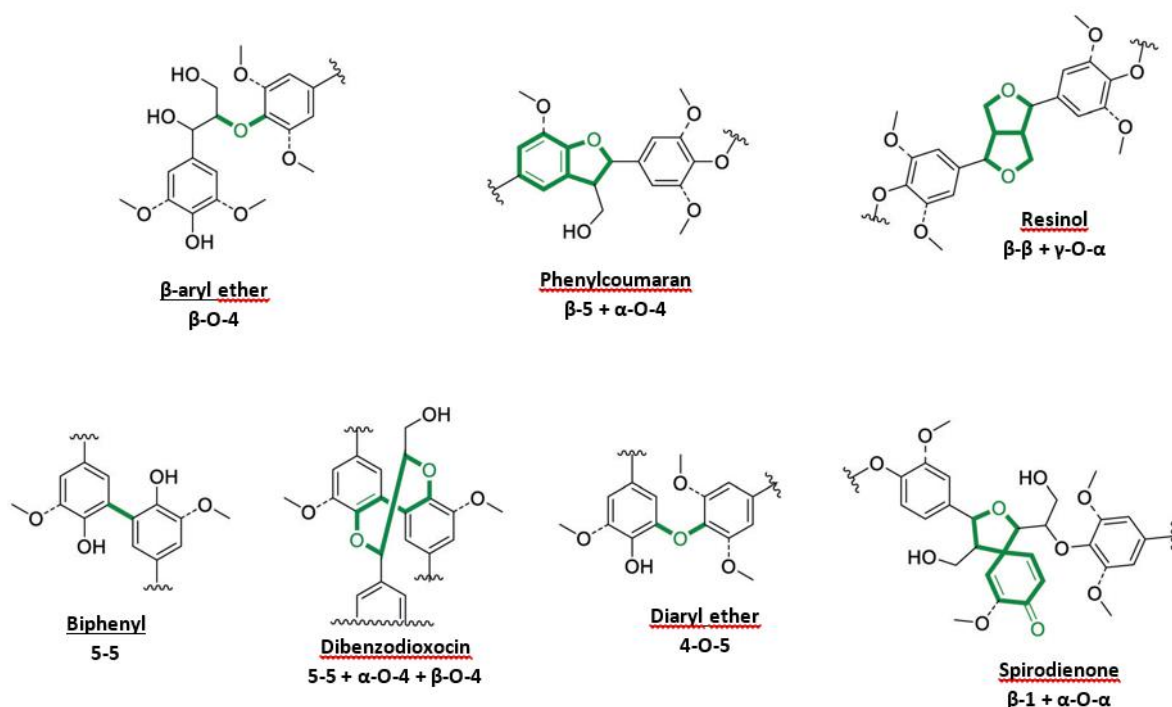
Figure 3: Representation of the most common bonding motifs in lignin (RINALDI ET AL., 2016).

Due to the apparently strong relationship between lignin structure and its properties, it is obviously important to gather valid structural information for an accurate characterization of different lignins. Nowadays, such investigational data can be obtained by a broad variety of non-destructive spectroscopic methods like solid-state nuclear magnetic resonance (SSNMR), vibrational (IR) or ultraviolet–visible (UV-Vis) spectroscopy. Furthermore, structural information can also be gathered by destructive techniques, using effectively a wide range of chemical degradation methods with a subsequent analysis of its degradation products. Comprehensive reviews on these methods were compiled by SARKANEN & LUDWIG (1971b); HEITNER, DIMMEL, & SCHMIDT (2010); and CALVO-FLORES ET AL. (2015). However, structural investigation is often applied to lignin isolated from the plant tissue. Since isolation—an essential step in sample preparation—is far away from being straightforward and mild, changes in both chemical composition and structure of the lignin must be expected to a certain degree. Nonetheless, there also exists a wide range of applicable methods, ranging from mechanical disintegration (i.e. milling) to chemical pulping and enzymatic processes. Again, a lot of literature is available reviewing the vast variety of usable methods (CALVO-FLORES ET AL., 2015; FENGEL & WEGENER, 1983; HEITNER ET AL., 2010; LAI & SARKANEN, 1971). The suitable isolation technique is usually chosen according to the purpose of separation, considering the desired quality or quantity of the obtained lignin. Generally, they can be divided regarding their approach: whether the lignin remains as insoluble residue or dissolves in an extraction solution. Regarding the first class of methods, oxidation or acidic hydrolysis of the polysaccharide fraction is carried out, leaving the lignin behind in high yields of over 80% (CALVO-FLORES ET AL., 2015).
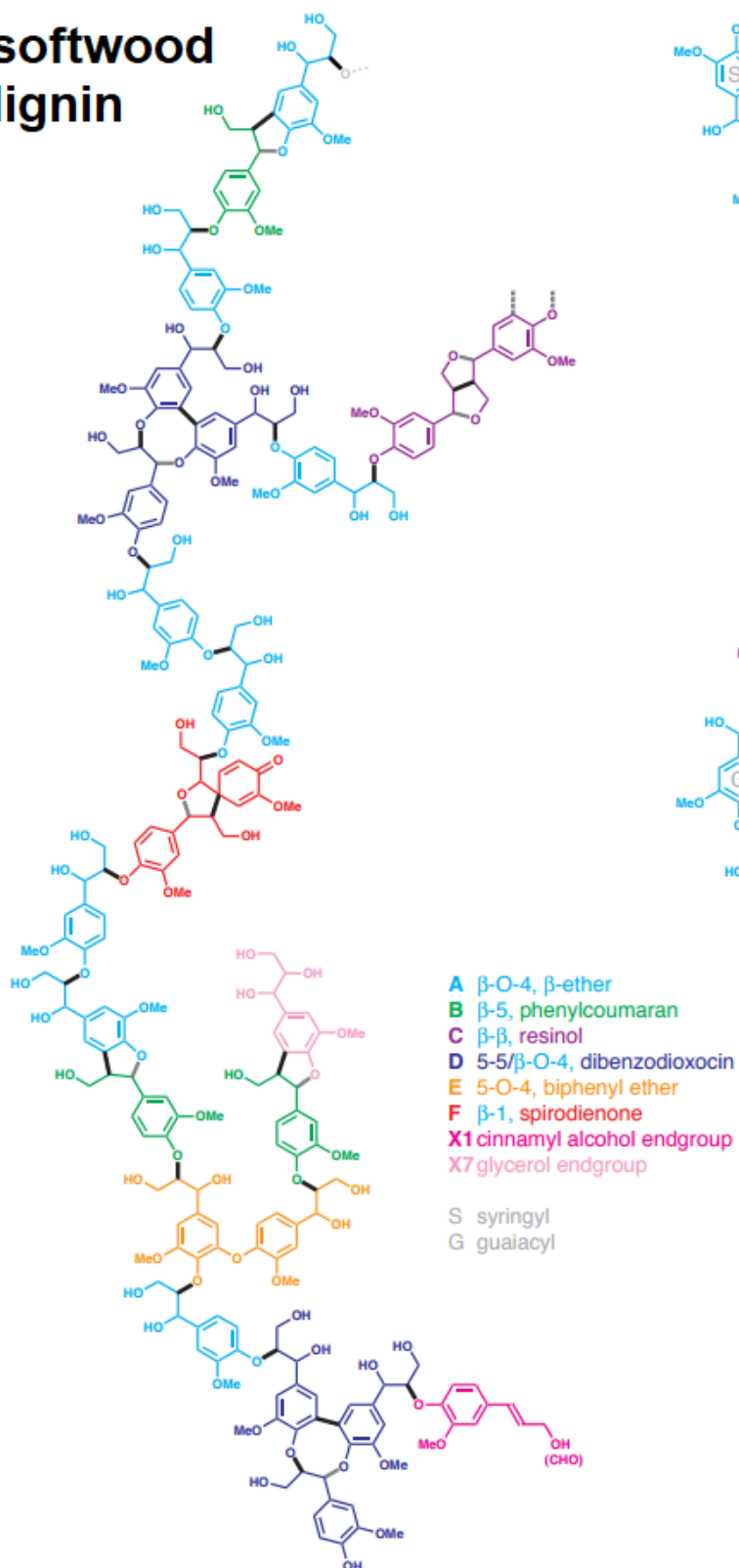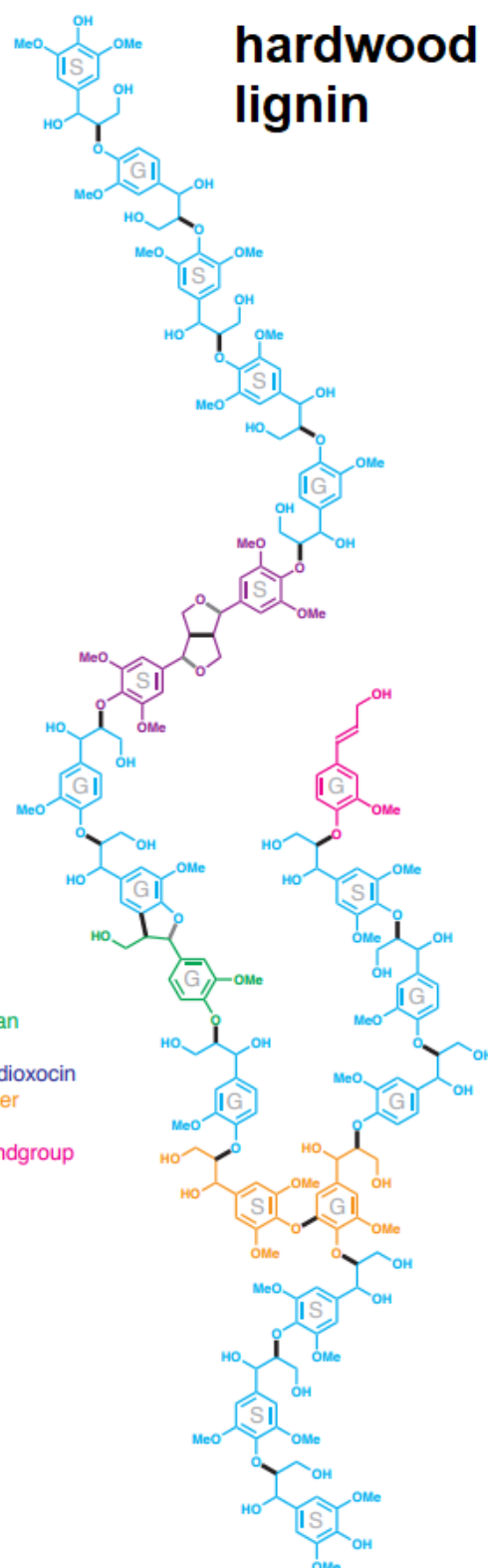
Figure 4: Lignin models for isolated softwood (spruce) and hardwood (poplar) lignins. Softwood lignins show a more compact structure due to branching (BOERJAN, RALPH, & BAUCHER (2003); BRUNOW (2005)).

Concerning the later methods, achieving a reasonable extraction of lignin, without altering its structure too much and in acceptable quantity, can be a very challenging task, since its solubility in common solvents is very poor (CALVO-FLORES ET AL., 2015). In laboratory-scale approaches, the extraction is usually carried out under mild and benign process conditions, often with the aid of auxiliary procedures like milling, cellulytic enzymes or steam-explosion (CALVO-FLORES ET AL., 2015). While these processes are designed to provide lignin, which can confidently be expected to resemble native lignin, commercially implemented large scale applications usually aim at a completely different target. There, the primary objective is the purification of polysaccharides, to produce suitable pulp for the manufacturing of paper and other related products. There, lignin is merely seen as by-product, and is mostly burned after separation as fuel for the paper mill. However, in respect of the size of the pulping industry, the amounts of modified lignin isolated are enormous and investigations on their properties are of huge interest for scientific and economic reasons.

1.1.1 Isolated lignin

Depending on the applied lignin removal technology, referred to as pulping, various modified lignins are formed showing quite different properties regarding solubility, reactivity and chemical composition. Basically, a distinction between sulfur and non-sulfur containing lignins from pulping procedures can be made; the sulfur containing ones are clearly dominating, deriving from either the sulfite or the Kraft (sulfate) process. Beside these two processes, only a few less popular pulping procedures are commercially in use.

Among these, extraction of lignin using organic solvents such as methanol, ethanol or acetic acid in aqueous solutions—so-called organosolv-lignin of both high purity and quality—receives a lot of attention, though a successful commercial application had failed so far (CALVO-FLORES ET AL., 2015).
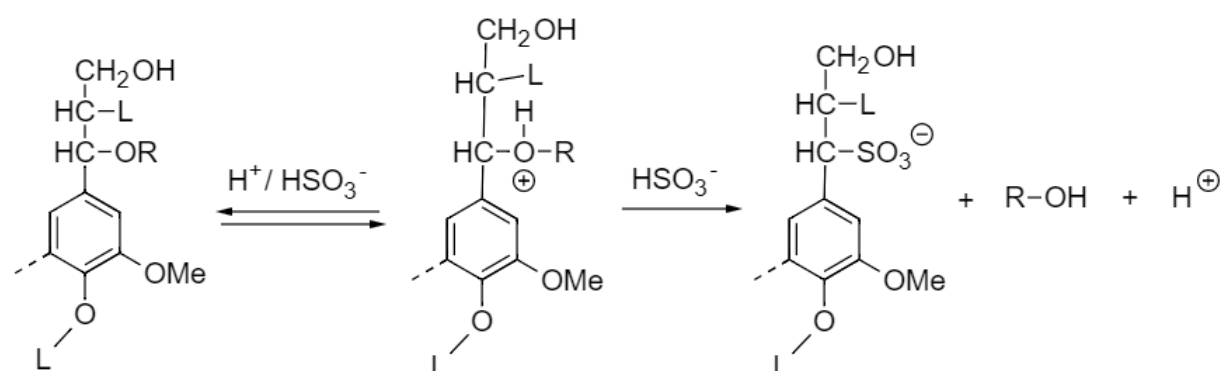

Figure 5: Mechansim for the sulfonation of lignin under acidic sulfite pulping conditions. L and R denote as lignin residues (GELLERSTEDT, 2009B).

For a long time, the most popular pulping process was the sulfite process, before it was overtaken by the Kraft process in the late 1940s (BIERMANN, 1996). Today, only a very small part of the world pulp production still relies on it (BRÄNNVALL, 2009). The removal of lignin from the polysaccharides in the sulfite process is based on the usage

of several salts of sulfurous acid, such as sulfides (S^{2-}) or bisulfides (HS^-). One of its main characteristics of this process is that it can be carried out at various pH levels from acidic to neutral and even alkaline, depending on the used (alkali) salts (Na^+, Mg^{2+}, Ca^{2+}, NH_4^+). When compared to Kraft pulp, sulfite pulp benefits from a higher yield, purity, water absorption capacity, brightness and a better bleachability, while suffering from weaker mechanical properties such as lower tensile strength (BIERMANN, 1996). Overall, the sulfite process also lacks in an effective recovery of cooking chemicals, which is either impossible (NH_4^+) or complicated (Na^+, Mg^{2+}) and impractical (Ca^{2+}); another important economic drawback compared to the Kraft process (BIERMANN, 1996). Next to acidic hydrolysis of ether linkages, dissolution of the lignin in sulfite pulping is achieved by introducing polar sulfonate groups (Figure 5), resulting in a drastic increase in water solubility (GELLERSTEDT, 2009B). Consequently, lignins isolated from the sulfite liquor after pulping are usually called lignosulfonates. Due to their amphiphilic behavior—originating in the sulfonation of the apolar lignin backbone—they are used as dispersing agent in various industries (GELLERSTEDT, 2009B).

1.1.1.1 Kraft lignin

Currently, the Kraft process is the globally dominating chemical pulping method with an annual production of approximately 130 million tons of pulp (RINALDI ET AL., 2016). In contrast to sulfite pulping, Kraft pulping is performed at strongly alkaline conditions (above pH 12), allowing to digest resin rich wood species, because of the sufficient saponification of acidic extractives in alkaline media (BIERMANN, 1996). Initially, alkaline pulping was carried out using only sodium or calcium hydroxide (NaOH or $Ca(OH)_2$) as cooking chemicals; This is known as the soda process, which has only limited use for non-wood fibers nowadays (CALVO-FLORES ET AL., 2015). The addition of sodium sulfide (Na_2S) as cooking chemical was an advancement, which caused a significant reduction of cooking time by accelerating lignin dissolution, thus sparing the cellulose fraction from severe alkaline degradation (BIERMANN, 1996). Therefore, Kraft pulps are usually characterized by their high strength, though bleachability and yield is usually lower than in the case of sulfite pulping (BIERMANN, 1996). In Kraft pulping, cooking is usually carried out in a batch digester for several hours at temperatures between 155 and 175°C (BIERMANN, 1996; CALVO-FLORES ET AL., 2015; GELLERSTEDT, 2009B). Up to 95% of the lignin are removed from the lignified plant tissue using the so-called "white" cooking liquor, which is an aqueous solution of NaOH and Na_2S in concentrations of about 1 M and 0.1 M, respectively (MARTON, 1971). Essential factors in the pulping procedure range from wood species; chip geometry; liquor to wood ratio; the H-factor, as a measure of cooking intensity; to the effective concentration of alkali and sulfur. Even minor changes in one of these parameters can have a major influence on the pulping outcome (BIERMANN, 1996).

During Kraft pulping, lignin degradation occurs mainly through the breakup of β-aryl ether linkages, providing a vigorous fragmentation and a sufficient introduction of

hydrophilic end groups for a successful solubilization of the lignin in the cooking liquor (GELLERSTEDT, 2009B). This decomposition reaction is initiated by the ionization of phenolic groups in the strong alkaline pulping environment, causing a simultaneous formation of quinone methide structures (Figure 6: Reaction scheme for the cleavage of β-aryl ether linkages during Kraft pulping. L denotes a lignin residue (GELLERSTEDT, 2009B).Figure 6) (DIMMEL & GELLERSTEDT, 2010). In presence of bisulfide (HS⁻) ions, quinone methide structures will form a thiol derivative at either the C-α or C-γ position, which in turn can perform a nucleophilic attack on the C-β, cleaving the β-aryl ether linkage (Figure 6). Afterwards, the formed instable episulfide degrades to elemental sulfur, which is rapidly converted to polysulfide and further back again to bisulfide (HS⁻) (DIMMEL & GELLERSTEDT, 2010). In the case of non-phenolic β-aryl ether structures, bisulfide (HS⁻) is not involved in the degradation process; it depends on ionized hydroxyl groups on the C-α or C-γ position, which can perform a nucleophilic attack on the C-β, leading to the cleavage of the β-aryl ether linkage (Figure 7) (DIMMEL & GELLERSTEDT, 2010).
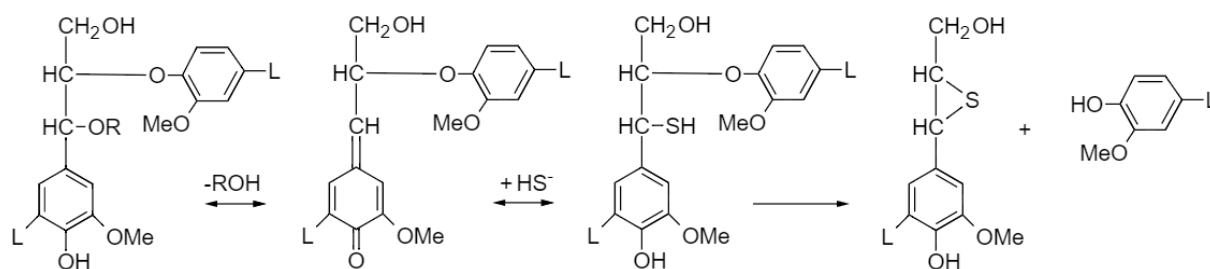

Figure 6: Reaction scheme for the cleavage of β-aryl ether linkages during Kraft pulping. L denotes a lignin residue (GELLERSTEDT, 2009B).

Unlike the vulnerable ether bonds, the covalent carbon to carbon linkages, especially the biphenyl linkage (Figure 3), remain largely unchanged. However, they can undergo a rearrangement, leading to stilbene structures (DIMMEL & GELLERSTEDT, 2010). Furthermore, alteration of end groups, concerning particularly the methoxy groups of guaiacyl and syringyl units, occurs to some extent (GELLERSTEDT, 2009B). Although the cleavage affects only approximately 1–2% of the present methoxy groups, the reaction with bisulfide (HS⁻) leads to the formation of volatile malodorous compounds like methyl mercaptan (CH_3SH), dimethyl sulfide (DMS) or dimethyl disulfide (DMDS), their restricted emission representing an important limitation factor for productivity in Kraft pulping (GELLERSTEDT, 2009B). Another undesirable side reaction is the formation of stable enol ether structures from the quinone methide intermediate, which are invulnerable for further degradation (DIMMEL & GELLERSTEDT, 2010; GELLERSTEDT, 2009B). Beside the fragmentation process, condensation reactions are likely to take place, since a lot of reactive structures prone to nucleophilic attacks, e.g. quinone methide, episulfide and epoxide structures, are present during Kraft pulping (DIMMEL & GELLERSTEDT, 2010). As a result, manifold alkaline stable condensation products are obtained (Figure 8), including newly formed C − C lignin bonds, and lignin to

carbohydrate bonds, constituting the so-called lignin-carbohydrate complexes (LCC) (DIMMEL & GELLERSTEDT, 2010).
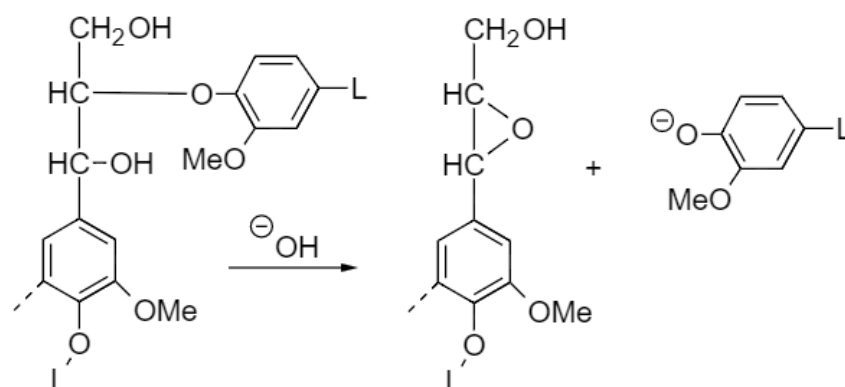

Figure 7: Mechanism for the cleavage of non-phenolic β-aryl ether structures during Kraft pulping (DIMMEL & GELLERSTEDT, 2010).

According to GELLERSTEDT (2009), delignification in Kraft pulping can roughly be divided into an initial, bulk and residual phase. In the initial phase, about 20% of the lignin dissolves into the liquor along with a substantial part of the polysaccharides, mostly hemicelluloses. Afterwards, a quite fast and selective lignin removal takes place in the bulk phase. In this phase, other catalysts than Na_2S—such as anthraquinone or polysulfide—are used to improve delignification rates. Thus, degradation of the cellulose fraction is avoided to some extent and the pulp yield is increased (DIMMEL & GELLERSTEDT, 2010; GELLERSTEDT, 2009B). Once approximately 90% of the lignin is removed, the residual phase begins, which is again characterized by a rather slow delignification rate compared to the degradation of polysaccharides. Thus, pulping is usually terminated as soon as this transition point is reached. Anyway, aggregation of lignin fragments in the liquor as well as condensation reactions, especially the formation of LCC's, tend to be more frequent in this final phase (DIMMEL & GELLERSTEDT, 2010).
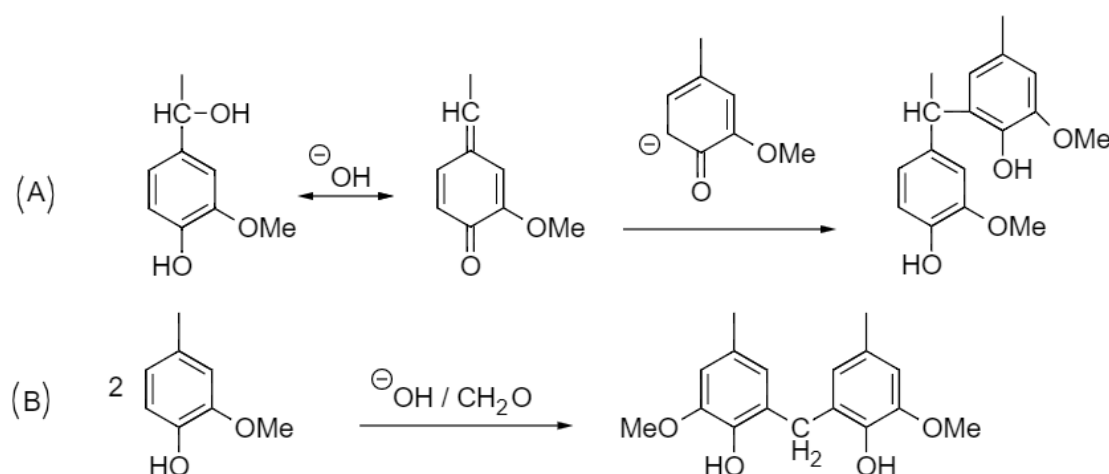

Figure 8: Suggested condensation reactions during alkaline pulping based on model compound studies: (A) addition of carbanions (B) formation of methylene bridges (DIMMEL & GELLERSTEDT, 2010).

Once the cooking process has reached its final delignification phase, it is terminated by washing the so-called "black" cooking liquor out of the pulp (BIERMANN, 1996). The "black" liquor consists of a vast variety of organic compounds accounting for about two thirds of its solids content, ranging from diverse fragmentation and degradation products of lignin or polysaccharides to saponified extractives. The remaining solids content is made up of inorganic substances originating mainly from the cooking chemicals, namely sodium and sulfur, which are accounting for about 20% and 5% of the "black" liquor solids content, respectively (MARTON, 1971). In normal operation, the "black" liquor is condensed up to a solids content of about 80% using a multi-stage evaporation process, increasing immensely its calorific value, before being burned in the recovery furnace. This provides thermal energy and leaves behind an inorganic melt almost ready for the regeneration of "white" cooking liquor (BIERMANN, 1996). Alternatively, Kraft lignin can be isolated from the "black" liquor for other purposes than thermal exploitation, making it available for chemical or material use. Although fractionation with organic solvents is basically possible and would also lead to high purity lignin, acidic precipitation is usually more common (CALVO-FLORES ET AL., 2015). Both organic or mineral acids can be used to lower the pH of the "black" liquor below 12, allowing the Kraft lignin to precipitate. As filtering of the precipitate is difficult, a two-step acidification is often preferred (MARTON, 1971). Recently, a novel approach on lignin precipitation and its subsequent filtering, the so-called LignoBoost process, has been developed and is considered a much promising procedure to extract lignin in high purity from black liquor (ZHU, WESTMAN, & THELIANDER, 2014). The major improvement made in the LignoBoost process is originating in the consideration of the influences from ionic strength, pH and temperature on lignin solubility, thus allowing the efficient production of considerable amounts of lignin in high purity and quality (DANG, BRELID, & THELIANDER, 2016; ZHU & THELIANDER, 2015; ZHU ET AL., 2014). The resulting precipitated Kraft lignin represents a major part of the aromatic fraction of the "black" liquor, while some aromatic compounds remain acid soluble, containing substances like lignin monomers, dimers and oligomers as well as degradation products like vanillin or vanillic acid (MARTON, 1971). The filtered and purified precipitate is usually dried and milled to form a free-flowing brown powder (CALVO-FLORES ET AL., 2015).

The quality and the composition of the obtained Kraft lignin is strongly influenced by the botanical origin of the pulped wood species, the actual pulping conditions and the chosen isolation method, so a wider dispersion of properties can be expected (MARTON, 1971). Nonetheless, some characteristics can be outlined. Although the content of hydroxyl groups remains overall nearly unchanged, a distinct shift from aliphatic to phenolic hydroxyl groups can be observed, where the dramatic increase in phenolic end groups, from originally 30 up to 70 phenolic units per 100 phenylpropane units, is largely caused by the massive cleavage of β-aryl ether linkages (DIMMEL & GELLERSTEDT, 2010; MARTON, 1971). But still, there can be found some residual β-aryl ether structures in softwood Kraft lignin, mostly preserved as non-phenolic β-aryl ether structures or alkali stable enol ether structures (DIMMEL & GELLERSTEDT, 2010). As already mentioned before, the more stable C – C linkages remain largely unchanged,

exhibiting only rearrangement (stilbene structures) to some extent. However, due to the various condensation reactions during the pulping process, a somewhat substantial amount of condensed structures deviating from the natural occurring C – C linkages can be expected (Figure 8), including LCC as well (DIMMEL & GELLERSTEDT, 2010). Furthermore, the content of certain functional groups is also affected by the pulping and isolation methods in diverse ways. As mentioned previously, 1–2% of the methoxy groups are split off during pulping, reducing its number to about 14 methoxy groups per 100 phenylpropane units in softwood Kraft lignin (MARTON, 1971). The number of carbonyl groups also decreases from about 20 to 15 carbonyl units per 100 phenylpropane units, while carboxylic groups are introduced in an amount of about 15 carboxylic units per 100 phenylpropane units (MARTON, 1971). Also, residual quinoid structures may be still present as well as sulfur containing functional groups, leading to a sulfur content of about 1.5% in Kraft lignin (CALVO-FLORES ET AL., 2015; MARTON, 1971). A model depicting the structural changes on lignin during Kraft pulping is shown in Figure 9.
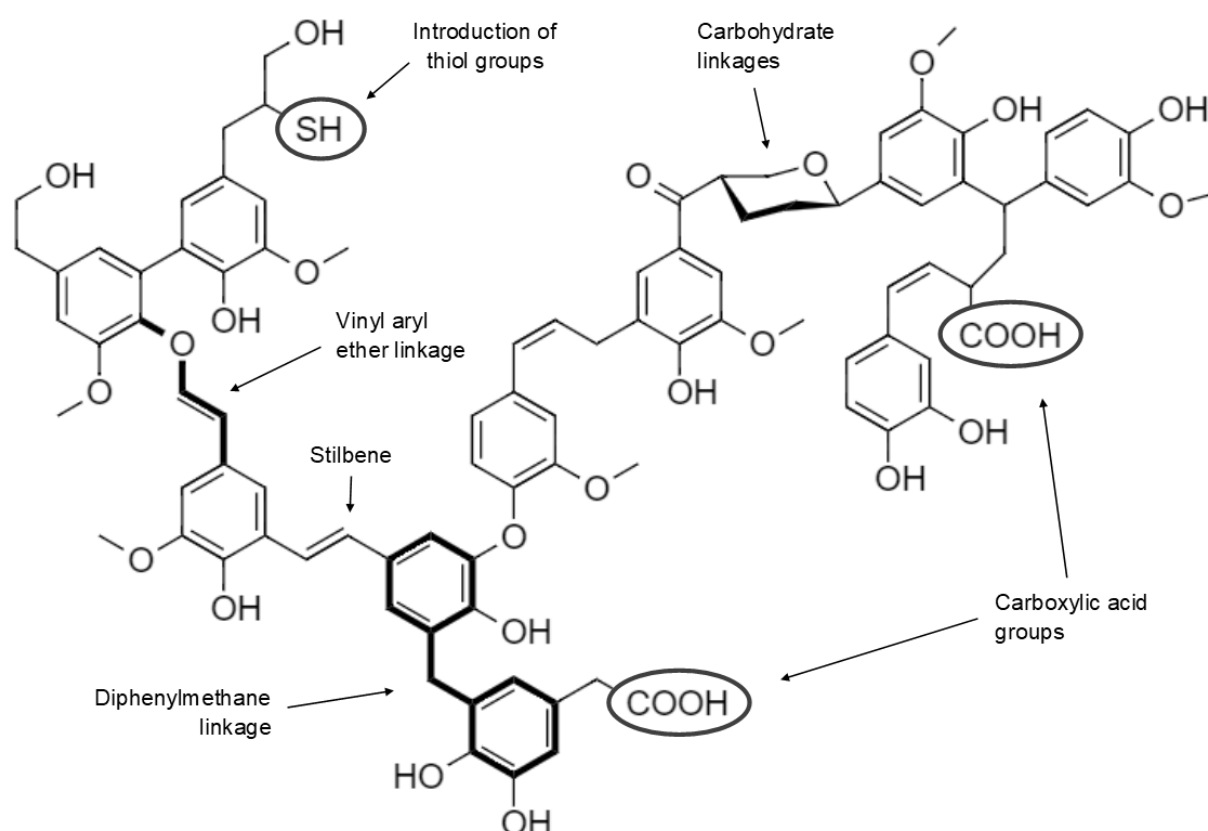

Figure 9: Model depicting the structural characteristics of Kraft lignin (adapted from ZAKZESKI, BRUIJNINCX, JONGERIUS, & WECKHUYSEN (2010))

In the comparison between different polymeric materials, the weight-average molar mass and the dispersity index are the most commonly used parameters, both describing the observed molecular weight distribution of the given polymer, allowing an approximate prediction of its physical properties. The weight-average molar mass

of Kraft lignin is obviously much lower than that of the original native lignin, usually ranging between 3 000 and 20 000, with a much higher dispersity index between 2 and 12, revealing once more its comparably heterogenous character (CALVO-FLORES ET AL., 2015). Concerning its thermal properties, Kraft lignin is behaving like a thermoplastic polymer with decomposition starting at temperatures around 200°C (MARTON, 1971). Due to its extraordinary structural composition, somewhat high molecular weight and disordered shape, solubility is limited in many solvents, thus leading rather steeply to high viscosities and gelling with increasing concentrations (CALVO-FLORES ET AL., 2015; MARTON, 1971).

1.1.2 Lignin utilization

Kraft lignin is still underutilized as resource for material use, despite its low-price, its availability in huge quantities and its apparent chemical value. In contrast, lignosulfonates are much more established in commercial use (CALVO-FLORES ET AL., 2015). However, the field of application can be expected as broad as it is in the case of lignosulfonates. Beside its primary use as fuel, Kraft lignin can also be subjected to chemical conversion such as gasification or depolymerization, resulting in either low value chemicals, like syngas, or high value chemicals, just like vanillin, DMS, or other substances known from similar biorefinery processes (CALVO-FLORES ET AL., 2015). The use of lignin in small quantities as an additive is already a popular application in many different economic sectors. Benefiting from its excellent suitability as dispersant, emulsifier, surfactant, floating or chelating agent, product performance can be efficiently improved. Furthermore, its non-toxicity and biodegradability make it also suitable for applications in the agricultural, fertilizer and feed industry, as well as in bioscience and medical research (CALVO-FLORES ET AL., 2015). One of the most promising approaches for the use of Kraft lignin in massive quantities is the use in the plastics industry, namely as copolymer and/or macromonomer, representing an important non-synthetic alternative. Nowadays, lignin is already used as precursor for carbon fibers, nanoparticles, hydrogels, foams and other composites, but it still has not made its breakthrough to conventional polymers, although it can enhance polymer properties like tensile strength, thermal stability or biodegradability (CALVO-FLORES ET AL., 2015). Partly, this is related to the non-standardized quality of the available lignin; however, its relatively low reactivity constitutes its major drawback. Targeting this specific problem, a vast variety of different modification methods are available to improve the competitiveness of lignin, ranging from addition of phenolic groups, hydrolyzation of methoxy groups to the introduction of new functional groups and heteroatoms (CALVO-FLORES ET AL., 2015). Among these methods, oxidative bleaching appears to be a quite suitable modification method for the pulp industry, since companies are already familiar with this kind of chemical process and technical equipment are often already available at the sites. Moreover, decoloration of the dark brown or black lignin is really a welcomed effect, further enhancing its scope of application in polymer industries.

1.2 Oxidative bleaching agents

1.2.1 Oxygen O$_2$

Nowadays, oxygen is a widely used bleaching agent in the pulp and paper industries. Whether as standalone bleaching stage or as reinforcement in extraction stages, it has proven its great usefulness, due to its relatively cheapness compared to other bleaching chemicals while it offers a sufficient bleaching effect (BIERMANN, 1996; CALVO-FLORES ET AL., 2015; GELLERSTEDT, 2009A; GERMGARD, 2009A).

Another advantage is the possible on-site production. Usually, pure oxygen is produced in massive quantities through air distillation, a cryogenic separation method, but since bleaching does not necessarily require high purity, a simpler and cheaper method—vacuum pressure swing adsorption (VPSA)—is preferred by the companies (GERMGARD, 2009B). In VPSA, air is streaming through a molecular sieve consisting of zeolite, which adsorbs nitrogen stronger than oxygen with increasing pressure (up to 7 bar), causing their separation (GERMGARD, 2009B). Once the molecular sieve is increasingly charged and separation efficiency is strongly declining, regeneration of the material is initiated by reducing the pressure; vacuum (0,3–1 bar) is applied to speed up the process (GERMGARD, 2009B). VPSA allows to produce 1–200 tons of oxygen per day in purities up to 90%, which is more than sufficient for the desired bleaching purposes (GERMGARD, 2009B).

Oxygen may be the least selective bleaching agent used in the pulp and paper industry, but when used in the right conditions, oxygen bleaching represents an efficient and cheap bleaching process. The oxygen bleaching stage (O-stage), also known as oxygen delignification, is usually performed right after the pulp washing, prior to the main bleaching stages. Oxygen delignification is carried out in a reaction tower at temperatures around 100°C for 20–60 minutes under alkaline conditions (final pH of 10–11) and an elevated oxygen partial pressure of about 700kPa, to ensure a higher solubility of oxygen in the bleaching solution (BIERMANN, 1996; GERMGARD, 2009A).
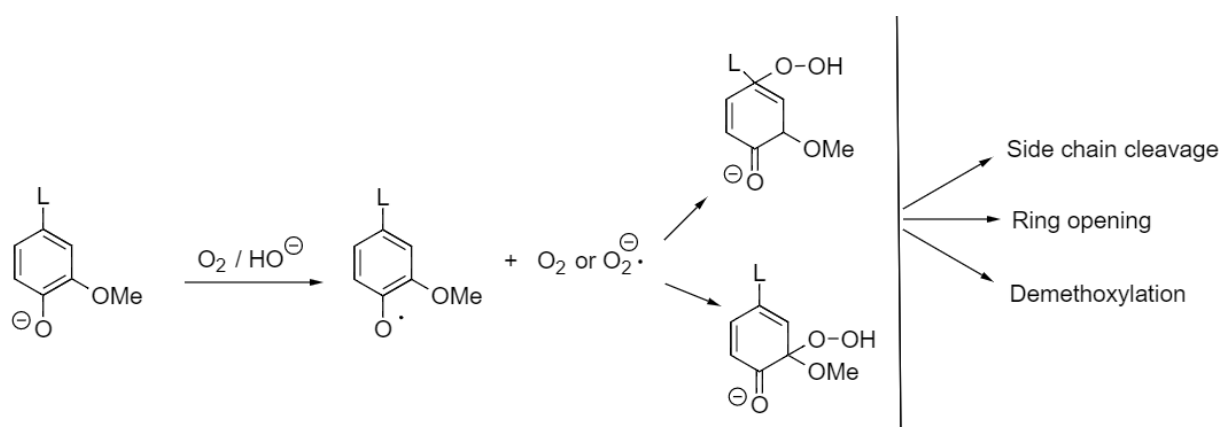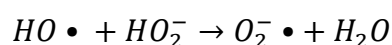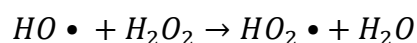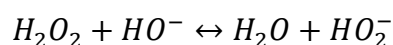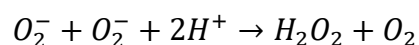

Figure 10: Oxidation mechanism in alkaline oxygen bleaching of lignin. The various modes of reaction are indicated on the right side. L denotes a lignin residue (GELLERSTEDT, 2010).
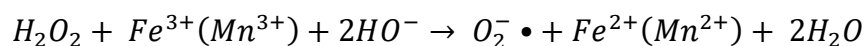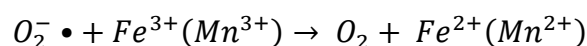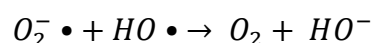
In oxygen delignification, phenolic units are playing an essential role in the oxidation mechanism, as under the alkaline conditions, lignin reactions are initiated by an

electron transfer from a phenolate anion to an oxygen molecule, leading to the formation of a phenoxy and a superoxide radical ($O_2^-\bullet$) (Figure 10). In the following, organic hydroperoxides are formed by the reaction of the superoxide radical ($O_2^-\bullet$) with a phenoxy radical in any of its mesomeric forms (GELLERSTEDT, 2010). The unstable hydroperoxide structures are further subjected to secondary reactions, including ring-opening, methoxy group or side group cleavage (GELLERSTEDT, 2010).

Overall, ring-opening reactions are dominating, leading to the massive formation of carboxylic end groups, i.e. muconic acid structures, and thus substantially increasing water solubility of the lignin (KALLIOLA, VEHMAS, LIITIÄ, & TAMMINEN, 2015; KUITUNEN ET AL., 2011). Additionally, the muconic acid like structures are acting as radical scavengers for hydroxyl radicals (HO•) and consume a lot of oxygen in their further degradation to carbon dioxide (CO_2), formic and oxalic acid (CHANG & ALLAN, 1971; KUITUNEN ET AL., 2011). Side chain cleavage is usually linked to the presence of an alcohol or carbonyl group in α-position (GELLERSTEDT, 2010). At pH levels above 12, enhanced introduction of α-carbonyl groups as well as rearrangement of the hydroperoxide structures occur, both strongly promoting side chain cleavage, leading to the increased formation of either phenolic aldehydes or quinoid structures (CHANG & ALLAN, 1971; GELLERSTEDT, 2009A, 2010; KALLIOLA ET AL., 2011; KUITUNEN ET AL., 2011; SIXTA, 2006). Furthermore, acetic or glycolic acid and vanillin are generated as a result of progressed degradation, serving well to estimate the degree of side chain degradation (CHANG & ALLAN, 1971; KUITUNEN ET AL., 2011).
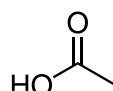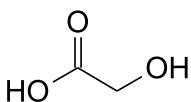
$$O_2^- + O_2^- + 2H^+ \rightarrow H_2O_2 + O_2$$

$$H_2O_2 + HO^- \leftrightarrow H_2O + HO_2^-$$

$$H_2O_2 + HO_2^- \rightarrow HO\bullet + O_2^-\bullet + H_2O$$

$$HO\bullet + H_2O_2 \rightarrow HO_2\bullet + H_2O$$

$$HO\bullet + HO_2^- \rightarrow O_2^-\bullet + H_2O \qquad\qquad \textbf{Equation 1}$$

$$O_2^-\bullet + HO\bullet \rightarrow O_2 + HO^-$$

$$O_2^-\bullet + Fe^{3+}(Mn^{3+}) \rightarrow O_2 + Fe^{2+}(Mn^{2+})$$

$$H_2O_2 + Fe^{2+}(Mn^{2+}) \rightarrow HO^- + HO\bullet + Fe^{3+}(Mn^{3+})$$

$$H_2O_2 + Fe^{3+}(Mn^{3+}) + 2HO^- \rightarrow O_2^-\bullet + Fe^{2+}(Mn^{2+}) + 2H_2O$$
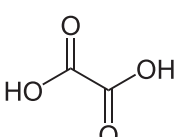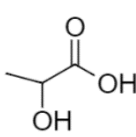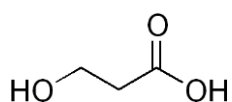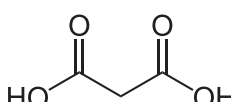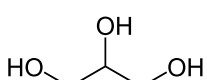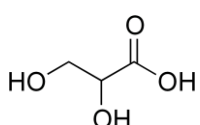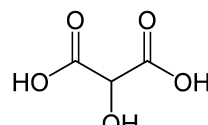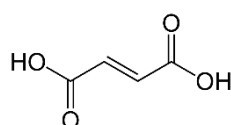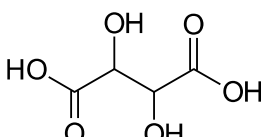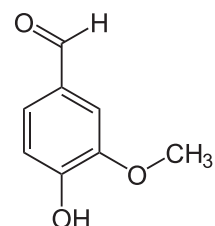
(according to GELLERSTEDT (2010))

In addition to the oxidation by the superoxide radical ($O_2^-\bullet$), a peroxide oxidation mechanism (see section 1.2.2 Hydrogen peroxide H2O2) must also be taken into consideration in oxygen delignification; hydroperoxyl radicals (H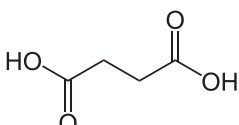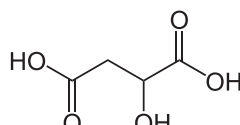O2•) can be generated in substantial amounts within the solution (Equation 1), resulting in deviating reaction pathways and degradation products (KUITUNEN ET AL., 2011). Therefore, a broad spectrum of final oxidation products can be expected from oxygen delignification. Depending on the intensity of the oxidative treatment, either aromatic intermediates or

low molecular weight aliphatic compounds are dominating (SUZUKI ET AL., 2006). In general, the aliphatic products can be divided in volatile compounds like methanol, formic or acetic acid, and non-volatile (hydroxylated) carboxylic acids like glycolic, oxalic, lactic, malonic, succinic, fumaric or malic acid, whereby formic, glycolic, acetic and oxalic acid are accounting by far for the largest share up to 90% of the total amount of acids (ROVIO ET AL., 2011; SUZUKI ET AL., 2006). A compilation of occurring organic compounds is given in Table 1.

Table 1: Compilation of organic compounds occuring during oxidative degradation of lignin

Organic compounds and their chemical structure

Methanol	Formic acid	Acetic acid	Glycolic acid

Oxalic acid	Lactic acid	3-Hydroxypropanoic acid	Malonic acid

Glycerol	Glyceric acid	Tartronic acid	Fumaric acid

Succinic acid	Malic acid	Tartaric acid	Vanillin

Beside the predominant degradation of phenolic units, other lignin structures are involved in the reaction mechanisms as well. Stilbene, styrene and catechol like structures as well as enol ether structures are highly susceptible to alkaline oxygen bleaching, leading to a somewhat selective degradation of these units, whereas non-phenolic β-aryl ether structures and condensed structures remain largely unaffected (GELLERSTEDT, 2010). As an alternative to the addition of a superoxide radical ($O_2^- \bullet$), preferably at pH levels below 12, condensed structures of the biphenyl type are continuously formed via a coupling reaction between two phenoxy radicals, leading subsequently to an increase in molecular weight (KALLIOLA, ASIKAINEN, TALJA, & TAMMINEN, 2014).

1.2.2 Hydrogen peroxide H$_2$O$_2$

In the pulp and paper industry, the main application area for hydrogen peroxide has been the bleaching of mechanical pulps. Here, solely the breakup of chromophoric structures, responsible for the dark coloring of the pulp, is intended, instead of a vigorous removal of the lignin, so that a profound brightening can be achieved without a severe loss of pulp yield (GERMGARD, 2009A). However, hydrogen peroxide is also increasingly applied in chemical pulp bleaching sequences. There, reaction temperatures are usually higher, around 100°C instead of about 70°C, and sodium silicate is added to stabilize the peroxide (GERMGARD, 2009A). Also, an upstream chelating stage (Q-stage) is often necessary to eliminate all types of transition metals, otherwise the peroxide would decompose (Equation 1) rather uncontrollably fast, leading to extremely poor bleaching results (GERMGARD, 2009A).

Unlike oxygen, hydrogen peroxide is almost exclusively produced off-site at big chemical companies. There, hydrogen peroxide is commonly produced using anthraquinone as catalyst, resulting in aqueous solutions with peroxide concentrations of 35–70% (GERMGARD, 2009B). Since hydrogen peroxide is highly prone to decomposition, exhibiting even explosive danger, storage is a serious matter. In order to maintain safety, storage tanks are often cooled, the pH of the peroxide solution is kept at 4–5 and stabilizers are also added (GERMGARD, 2009B).
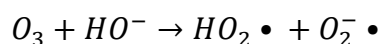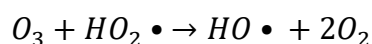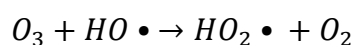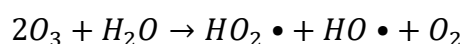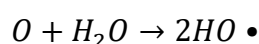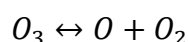
Like oxygen delignification, hydrogen peroxide bleaching (P-stage) is usually carried out under alkaline conditions, typically resulting in a final pH of 10–11 (GERMGARD, 2009A). Thereby, hydroperoxyl radicals (HO$_2$•) are constantly generated (Equation 1), which are showing similar reactions with organic substrates as the superoxide radical (O$_2^-$•) (See section 1.2.1 Oxygen O2), leading also to either ring-opening or side chain cleavage (GELLERSTEDT, 2009A; KUITUNEN ET AL., 2011; LEARY & SCHMIDT, 2010). Additionally, by the readily decomposition of either hydrogen peroxide (H$_2$O2) or hydroperoxyl radicals (HO$_2$•) (Equation 1) highly reactive hydroxyl radicals (HO•) are formed, which are exhibiting a very strong oxidizing potential of 2.0 V vs SHE (standard hydrogen electrode) (LEARY & SCHMIDT, 2010). Obviously, the hydroxyl radicals (HO•) are strongly interacting with lignin, exposing three main reaction ways: the addition of hydroxyl groups to unsaturated bonds (I), the abstraction of an electron from phenolate ions (II) and the abstraction of hydrogen (III) (GELLERSTEDT, 2010; LEARY & SCHMIDT, 2010). Consequently, oxidative ring-opening reactions and side chain cleavage is heavily promoted, followed by further oxidative degradation, giving rise to a broad spectrum of organic acids, including formic, glycolic, 3-hydroxypropanoic and 3,4-dihydroxybutanoic acid (GELLERSTEDT, 2009A) as well as acetic, oxalic, succinic and malonic acid (CALVO-FLORES ET AL., 2015). A compilation of occurring organic acids is given in Table 1.

1.2.3 Ozone O$_3$

1.2.3.1 Pulp and paper bleaching

Even though ozone is one of the strongest oxidizers, as it exhibits an oxidizing potential of 2.07 V vs SHE (HORVÁTH, BILITZKY, & HÜTTNER, 1985), it is rather seldomly applied in pulp and paper bleaching. However, it plays a significant role in the performance of total chlorine free bleaching sequences (GERMGARD, 2009A).

Since ozone rapidly self-decomposes to oxygen shortly after generation, storage is usually avoided and ozone production is always implemented on-site right next to the bleaching reactors (GERMGARD, 2009B). Typically, the corona discharge technique is used for ozone generation, which can be carried out using either air or pure oxygen, with oxygen being usually preferred (GERMGARD, 2009B). In any case, an oxygen containing gas stream is passing an electric discharge gap, where some of the oxygen molecules become excited and subsequently are converted to ozone (HORVÁTH ET AL., 1985; RICE, 1986). Using this method, gas streams with an ozone concentration of about 6–14% can be achieved (GERMGARD, 2009B).

$$O_3 \leftrightarrow O + O_2$$
$$O + H_2O \rightarrow 2HO \bullet$$
$$2O_3 + H_2O \rightarrow HO_2 \bullet + HO \bullet + O_2$$
$$O_3 + HO \bullet \rightarrow HO_2 \bullet + O_2$$
$$O_3 + HO_2 \bullet \rightarrow HO \bullet + 2O_2$$
$$O_3 + HO^- \rightarrow HO_2 \bullet + O_2^- \bullet$$

Equation 2

(according to BABLON ET AL. (1991); GELLERSTEDT (2010))

In contrast to oxygen or hydrogen peroxide, ozone bleaching (Z -stage) is performed at weakly acidic conditions (pH 2–3), due to the rapid self-decomposition of ozone in alkaline solutions (Equation 2) (GERMGARD, 2009A). Moreover, process temperatures are also lower (30–60°C), slowing down the rate of self-decomposition and increasing the solubility of ozone in the bleaching solution (GERMGARD, 2009A; HORVÁTH ET AL., 1985). Depending on pulp consistency, pressure up to 10 bar can be applied, thereby increasing the amount of dissolved ozone (GERMGARD, 2009A). Although achieving a sufficient dissolution of the ozone gas in the aqueous bleaching solution is not trivial, it is still much easier than it is in the case of oxygen, because of its much higher solubility (approximately 13 times higher) (HORVÁTH ET AL., 1985). Another striking characteristic is the extremely short process time in ozone bleaching, usually in the range of seconds to one minute (GERMGARD, 2009A).

As mentioned before, self-decomposition of ozone is greatly accelerated under alkaline conditions. Especially with increasing temperature, ozone can be expected to decompose almost immediately (HORVÁTH ET AL., 1985). This gives rise to the massive formation of superoxide radicals ($O_2^- \bullet$), hydroperoxyl ($HO_2 \bullet$) and hydroxyl radicals

(HO•) (Equation 2), and therefore oxygen and peroxide oxidation mechanisms (See sections 1.2.1 Oxygen O2 and 1.2.2 Hydrogen peroxide H2O2) can be assumed to occur (GELLERSTEDT, 2009A). As it is the case for oxygen and hydrogen peroxide, the presence of transition metals also promotes the formation of reactive oxygen species (GELLERSTEDT, 2010).
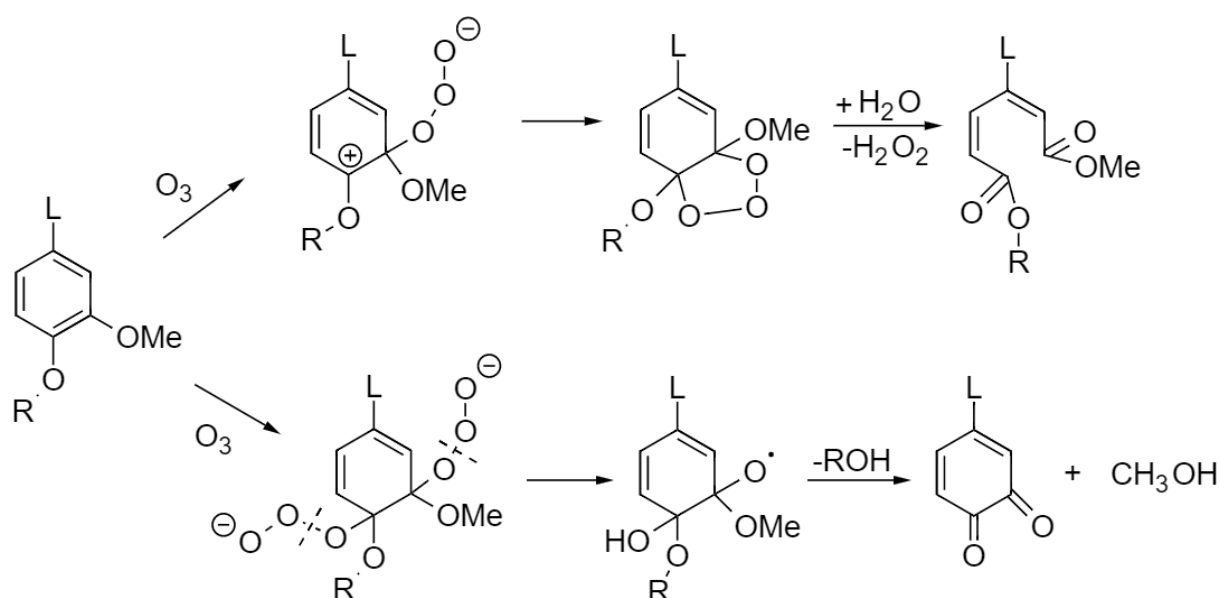

Figure 11: Ozone oxidation mechansim of lignin. Upper part: ring-opening reactions according to the Criegee mechanism. Lower part: addition of hydroxy groups and formation of quinoid structures. L and R are denoting lignin residues (adapted from GELLERSTEDT, 2009A).

Due to the lack of hydroxyl anions (HO⁻), ozone is much more stable at lower pH levels, allowing it to take part in the reactions as intact molecule (GELLERSTEDT, 2010). In the ozone oxidation mechanism, three different types of action can occur: cyclo addition (the so-called Criegee mechanism), electrophilic reactions, and nucleophilic reactions (BABLON ET AL., 1991). In cyclo addition, ozone is added to an unsaturated bond, leading to the formation of an ozonide intermediate, which is rapidly fragmented into carbonyl containing reaction products (Figure 11) (BABLON ET AL., 1991; GELLERSTEDT, 2010; HORVÁTH ET AL., 1985). The original unsaturated C – C bond is broken in this process. Electrophilic and nucleophilic reactions are promoted by the presence of either electron donating or withdrawing groups, leading to the addition of hydroxy groups, which further increases the reactivity towards ozone (BABLON ET AL., 1991; HOIGNÉ & BADER, 1983A). Overall, the ozone oxidation mechanism is practically limited to unsaturated bonds and is strongly influenced by specific functional groups present on the aromatic or olefinic molecule (BABLON ET AL., 1991; HOIGNÉ & BADER, 1983A, 1983B). During ozone oxidation, the aromatic ring structures of lignin are successively loaded with hydroxyl groups, transformed to muconic acid structures and finally degraded to aliphatic dicarboxylic acids, as it has been demonstrated for catechol (GELLERSTEDT, 2010). Interestingly, syringyl units show higher reactivity compared to guaiacyl and *p*-hydroxyphenyl units (GELLERSTEDT, 2010). Due to the selective attack on unsaturated bonds, the aliphatic side chains remain largely unaffected from oxidation by molecular ozone, but still the formation of phenoxy and superoxide (O₂⁻•)

or hydroxyl radicals (HO•) massively occurs during ozone bleaching, consequently leading to an unspecific oxidative degradation (GELLERSTEDT, 2010).

1.2.3.2 Effluent treatment

The strong oxidizing potential of ozone itself, combined with the formation of even stronger oxidizing hydroxyl (HO•) and hydroperoxyl radicals (HO₂•), causes a fast and unspecific degradation of almost every (high molecular) organic substance. This is the very reason for its emerging exploitation not only in public water purification and disinfection, but also in several effluent treatments (BABLON ET AL., 1991; RICE, 1986). A lot of research has been conducted on ozone processes for water and wastewater treatments (GOGATE & PANDIT, 2004; LANGLAIS, RECKHOW, & BRINK, 1991). Effluent treatments are usually aiming at the removal of chemical oxygen demand (COD), total organic carbon (TOC), color, adsorbable organic halides (AOX), as well as increasing biodegradability of the residuals (LANGLAIS ET AL., 1991). While color removal is easily achievable using ozone, due to its selectiveness towards unsaturated bonds present in chromophoric structures, reduction of COD and TOC is unfortunately limited. This is usually compensated by the increase of biodegradability of the residual oxidation products (GOGATE & PANDIT, 2004). In many cases, a combination of ozone with hydrogen peroxide, UV radiation or certain catalysts is applied to increase treatment efficiency regarding the removal of COD and TOC, as they all promote the formation of hydroxyl radicals (HO•) and thus improving the unspecific degradation of organic matter (GOGATE & PANDIT, 2004). These hybrid processes, referred to as Advanced Oxidation Processes (AOP), are typically considered as tertiary treatments to remove the last remaining recalcitrant water pollution (ALVARES, DIAPER, & PARSONS, 2001; GOGATE & PANDIT, 2004).

Despite the huge efforts to close water cycles, the pulp and paper industries are still representing a major source of wastewater. As environmental regulations concerning water pollution are getting stricter, meeting up with the enforced quality standards for discharged wastewaters demands new and more intensive strategies for wastewater treatments (KARAT, 2013). Consequently, ozone processes come to the fore, as they represent a reasonable alternative especially for effluents containing large amounts of aromatic and unsaturated compounds. Therefore, several companies have already implemented ozone processes in their wastewater treatment facilities (KARAT, 2013). However, large scale implementations are challenged by the expensive ozone generation with its huge demand of either moisture-free air or pure oxygen. Therefore, providing an efficient mass transfer of the ozone gas into solution, thereby minimizing the overall ozone demand, is a critical task in process control (KARAT, 2013). Keeping ozone consumption as low as possible while achieving a sufficient degree of oxidation to avoid toxic intermediates, is also a very difficult balancing act, but nonetheless essential for process efficiency (GOGATE & PANDIT, 2004; KARAT, 2013).
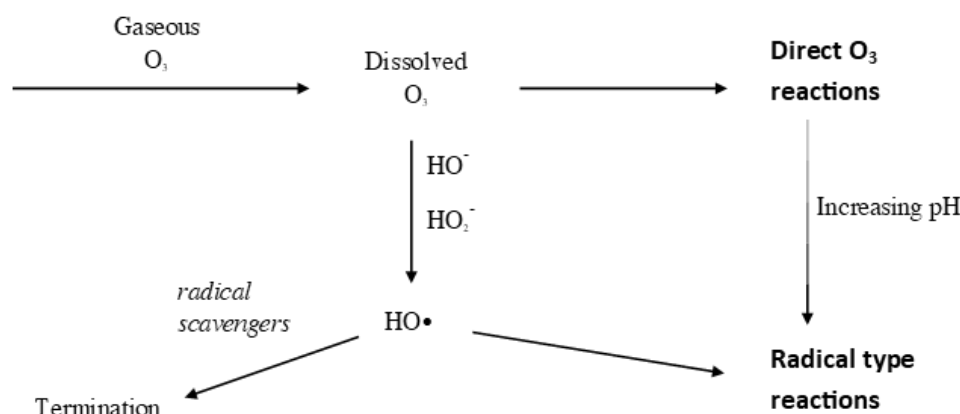
Figure 12: General scheme of the ozone oxidation mechanism in aqueous solutions; direct vs. radical type reactions (adapted from ALVARES ET AL. (2001).

Targeting these problems, a lot of research has been conducted to determine the optimum process conditions for the treatment of pulp mill effluents with solely ozone or in combinations with other techniques (CATALKAYA & KARGI, 2007; DE LOS SANTOS RAMOS, POZNYAK, CHAIREZ, & CÓRDOVA R., 2009; V. FONTANIER, BAIG, ALBET, & MOLINIER, 2005; VIRGINIE FONTANIER, FARINES, ALBET, BAIG, & MOLINIER, 2006; KREETACHAT ET AL., 2007; LEI & LI, 2014; MERAYO, HERMOSILLA, BLANCO, CORTIJO, & BLANCO, 2013; YEBER ET AL., 1999).

Summing up, ambient to slightly elevated temperatures are preferred, keeping the balance between ozone solubility and reaction rate, and moreover, maintaining low process costs. Optimum for pH has been experienced around 7–8, allowing both degradation pathways, direct and via radical formation (Figure 12) to occur, achieving maximum color abatement as well as maximum COD and TOC removal (ALVARES ET AL., 2001; GOGATE & PANDIT, 2004; LEI & LI, 2014). In addition, slightly alkaline to neutral conditions improve the formation of biodegradable intermediates, while strongly acidic conditions tend more to mineralization and show deficits in COD and TOC removal (ALVARES ET AL., 2001; BIJAN & MOHSENI, 2005; DE LOS SANTOS RAMOS ET AL., 2009; MERAYO ET AL., 2013). On the other hand, highly alkaline conditions massively increase ozone consumption as self-decomposition is taking place at very high rates, and therefore color removal is reduced to some extent (MERAYO ET AL., 2013).

Depending on the actual composition of the effluent, the exact process conditions, and the technical realization of the gas inlet, the required ozone dosage can vary greatly to achieve maximum COD and TOC removal. Indications are given by MERAYO ET AL. (2013), reporting a demand of 2.38 mg of ozone per mg of removed COD in a Kraft pulp mill effluent and by KO ET AL. (2009), using a dosage of 3 g/l ozone for their kinetic model experiments with pulp mill effluents.

Anyways, TOC removal is characterized by an initially high reaction rate, affecting especially less complex structures, leading to the rapid formation of oxidized degradation products, mainly aliphatic dicarboxylic acids like fumaric, maleic, malonic or formic acid (DE LOS SANTOS RAMOS ET AL., 2009), followed by a gradual slowdown in the reaction rate (KREETACHAT ET AL., 2007). The main reason for this slowdown is that

unsaturated (chromophoric) structures are increasingly competing with the accumulating amounts of aliphatic dicarboxylic acids, which also show a much higher resistance towards oxidation and thus effectively limit the total TOC removal (HOIGNÉ & BADER, 1983A, 1983B; KREETACHAT ET AL., 2007; LEI & LI, 2014). Furthermore, due to the permanent formation of dicarboxylic acids, the pH level is continuously lowered during the process, leading to a lower formation of hydroxyl radicals (HO•); as they exhibit a faster reaction rate than ozone towards organic substrates, overall degradation slows down (BIJAN & MOHSENI, 2005). Additionally, lower pH levels also result in a slower degradation of phenolic units, as the degree of dissociation of the hydroxyl groups governs the reaction rate (HOIGNÉ & BADER, 1983B). The generation of CO_2 in the oxidative degradation does not only contribute to a lowering in pH, the carbonate (CO_3^{2-}) and bicarbonate anions (HCO_3^-) also act as radical scavengers for hydroxyl radicals (HO•), further slowing down degradation (HOIGNÉ & BADER, 1983A; KARAT, 2013; LEI & LI, 2014).

Even though in progressed oxidation degradation to small aliphatic compounds and finally mineralization is occurring in a substantial amount, causing a significant shift in the molecular weight distribution towards low molecular compounds, high molecular weight compounds can still be present to a distinct degree after the treatment (BIJAN & MOHSENI, 2005). In part, this can be explained by the promptly decreasing reaction rate as size and complexity of the compound increases, leading to a significant higher residence time of high molecular weight compounds (BELTRAN-HEREDIA, TORREGROSA, DOMINGUEZ, & PERES, 2001). In addition, the high molecular weight fraction shows to some extent resistance against oxidative degradation (BIJAN & MOHSENI, 2005; V. FONTANIER ET AL., 2005).

1.2.3.3 Lignin bleaching

Although, a few reports on the modification of technical lignins like Kraft lignin or lignosulfonates with ozone have been published, surprisingly little literature is available on the chemical characterization of the ozonated lignin solutions, except for WANG, CHEN, & GRATZL (2004). In their work, purified pine Kraft lignin was dissolved in a 1 M NaOH solution in a concentration of 10 g/l. Subsequently, ozonation was carried out at ambient temperatures, using an ozone-air stream with an ozone concentration of 2–2.5%. In the following chemical characterization of the ozonated preparations, a few important insights on the degradation of lignin in alkaline solution by ozone were gained. The observed significant increase in solubility of lignin, despite the lowering of pH from 12.5 to 7 with progressing ozonation, was traced back to the initial high formation of carboxylic functional groups (from 0.5 to 3 mmol/g), preferably occurring at pH levels in the range from 12.5 to 10, when superoxide radicals (O_2^- •) and hydroperoxyl anions (HO_2^-) are the main reactive species. Additionally, the declining amount of phenolic and aliphatic hydroxyl groups (from 8 to 5 mmol/g) indicated a vigorous degradation of side chains, leading to the formation of carbonyl and quinoid structures, as well as ring-opening reactions at this pH range. The later was further

confirmed by the reduction of methoxy groups (from 4 to 3 mmol/g). But as pH dropped below 9, the hydroperoxyl ($HO_2\bullet$) and hydroxyl radicals ($HO\bullet$) became predominant, leading to an increase in hydroxylation of aromatic rings and condensation reactions between fragmented lignin moieties. As a result, a steady increase in the weight-average molar mass from 5500 to 10,100 was observed as ozonation progressed. In addition, a distinct shift in the molecular weight distribution towards the high molecular weight fraction was observed, caused by the strong degradation of the low molecular weight fraction at high pH levels and by the promoted condensation reactions at nearly neutral pH levels.

1.3 Analytical methods

1.3.1 Ultraviolet–visible spectrophotometry (UV-Vis)

The absorption of electromagnetic radiation in the range of ultraviolet and visible light is based on the molecular electronic transition of π or non-bonding electrons, allowing to link molecular structure with the absorption at a specific wavelength (SCHWEDT, 2008). Beside qualitative analyses, it is also possible to gain quantitative information in UV-Vis spectrophotometry, as—according to the Lambert–Beer law (Equation 3)—in diluted solutions the absorbance is directly proportional to the concentration of the absorbing species.

$$A(\lambda) \ = \ \log\left(\frac{I_0}{I_1}\right) = \ \varepsilon_\lambda \ \cdot c \ \cdot L$$

$A(\lambda)$ ...   *absorbance at wavelength λ*

I_0 ...   *intensity of incident light*   **Equation 3**

I_1 ...   *intensity of transmitted light*

ε_λ ...   *molar attenuation coefficient at wavelength λ*

c ...   *concentration of absorbing species*

L ...   *path length through sample*

Naturally, UV-Vis spectroscopy is very common for color measurements, i.e. in wastewater facilities, color is usually defined as the absorption at 465 nm (BIERMANN, 1996). In pulp and paper industries, the brightness (yellowness) of a paper surface is defined as the absorption at 457 nm (BIERMANN, 1996).

Absorption around 400 nm corresponds to carbonyl and quinoid structures, allowing to estimate their concentration to some extent (GELLERSTEDT, 2010; SCHMIDT, 2010). Due to the aromatic structure of lignin, absorbance in the UV range is very strong, revealing two maxima at approximately 200 and 280 nm, followed by a gradual decrease towards the visible range of the spectra (Figure 13). Therefore, lignin concentration is usually referred to the absorbance at 210 or 280 nm (CALVO-FLORES ET AL., 2015).
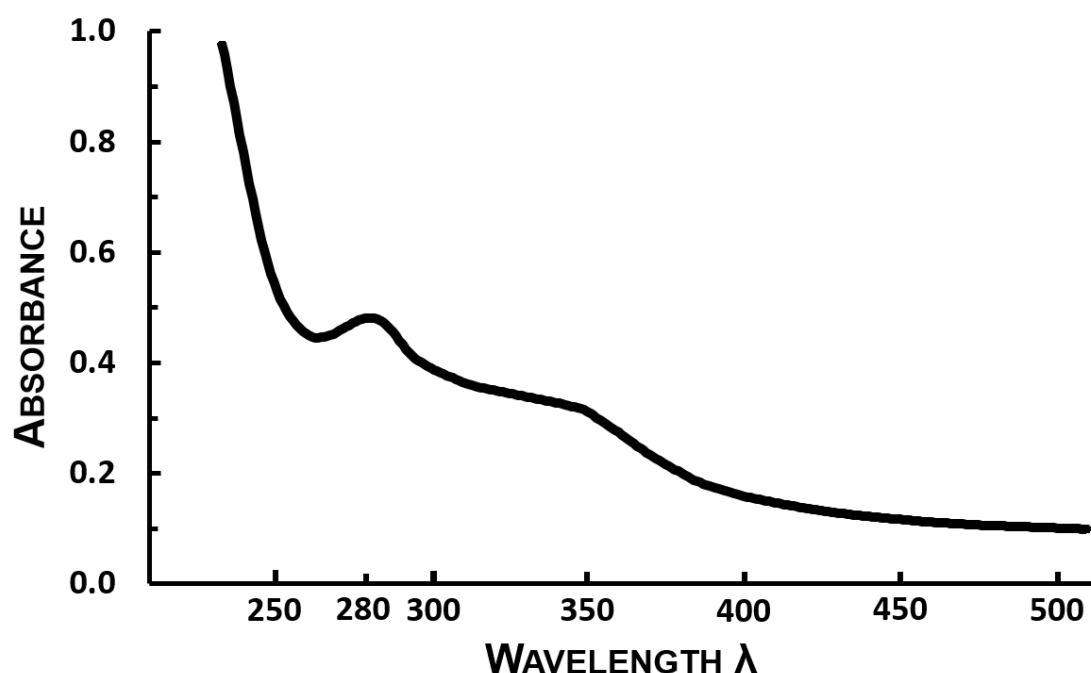
Figure 13: UV-Vis spectra of Kraft lignin in solution.

As the obtained lignin spectra represents the sum of all it constituents, information on its composition can be drawn from spectral analyses. In many cases, comparing the absorption spectra before and after a specific chemical treatment is helpful to accurately interpret the spectral data (SCHMIDT, 2010). Frequently used techniques are ionization of phenolic groups and reduction by borohydride, leading to a noticeable shift in the obtained spectra to longer or shorter wavelengths, respectively (GOLDSCHMID, 1971).

1.3.2 Non-purgeable organic carbon (NPOC)

The total amount of dissolved organic carbon is typically of great interest in effluent analytics, since it is considered a valid indicator for water pollution and contamination. The determination is usually designed as two-stage process; yielding the organic carbon content as difference between the total and the inorganic carbon content. In contrast, direct methods apply sample pretreatments to eliminate the inorganic carbon before measuring the total carbon content (GREENBERG, 1992).

In non-purgeable organic carbon measurement, inorganic carbon as well as volatile (purgeable) organic carbon is eliminated by acidification and sparging the sample with carrier gas. The remaining organic carbon is then catalytically oxidized in a combustion tube to create CO_2. Subsequently, the combustion gas is cooled and dehumidified, before the generated CO_2 is detected by a nondispersive infrared detector (NDIR) for quantification (GREENBERG, 1992).

1.3.3 Chromatography

The term "chromatography" refers to a vast number of physicochemical separation processes, which are exploiting the differential partitioning of compounds between a stationary and a mobile phase (SCHWEDT, 2008). In general, interactions between compounds and the stationary phase slow down the flow of the analytes in the mobile phase, causing an overall separation of the different constituents of a mixture, due to the resulting divergent retention times (SCHWEDT, 2008). Usually, chromatography methods are distinguished by the design of the stationary phase (planar or column) and by the physical state of the stationary (solid or liquid), and of the mobile (liquid or gas) phase. In addition, chromatography can be performed either on preparative or analytical scale.

1.3.3.1 Gas chromatography (GC)

The schematic layout of a gas chromatograph is displayed in Figure 14. In GC, the separation is always carried out in columns, containing a packed or film stationary phase, using an inert carrier gas like helium, argon or nitrogen as the mobile phase. Here, vapour pressure takes over the leading role in the separation, albeit the polarity of the stationary phase is still having an influence on the partition equilibrium (SCHWEDT, 2008).
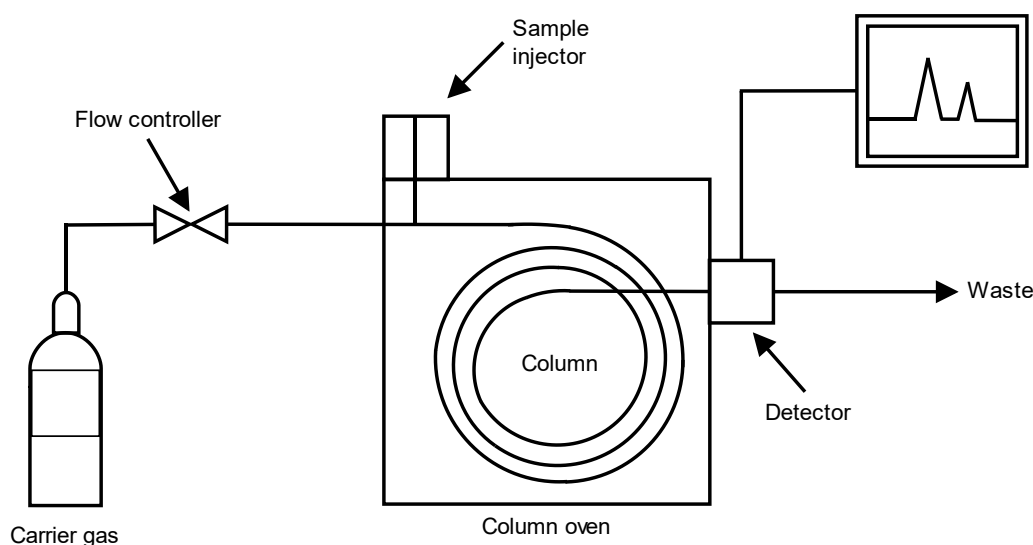

Figure 14: Schematic diagram of a gas chromatograph.

1.3.3.2 Mass spectroscopy (MS)

The principle of MS is based on the ionization of chemical species in a gaseous sample, causing fragmentation of the generated ions. Subsequently, the fragments are separated due to their mass-to-charge ratio by accelerating them in an electric or magnetic field (HÜBSCHMANN, 2001). The resulting mass spectrum, a plot of the relative abundance of the ion signal as a function of the mass-to-charge ratio, is further used

for the identification of the compound, as the fragmentation patterns are characteristic for certain chemical structures (SCHWEDT, 2008).

Among the several available implementations for the ionization procedure, the standard technique for hyphenation to GC is the electron impact ionization. The inflowing gas is fired at by electrons to generate charged ions (HÜBSCHMANN, 2001).

Nowadays, the filtering of the charged ions (fragments) according to their mass-to-charge ratio, is often carried out by a quadrupole mass analyzer. Here, filtering is achieved by an oscillating high-frequency electric field, which is generated by four cylindrical rods, set parallel to each other (SCHWEDT, 2008).

2 Objective of the diploma Work

The aim of this study was to characterize the chemical effects during modification of Kraft lignin with ozone under alkaline conditions.

The question of interest was what are the effects of the initial pH on the modification process. For this purpose, three experiments varying in alkalinity (0.2, 0.4 and 1 M) were carried out. Furthermore, fractionation was performed on the modified samples— including acidic precipitation and resin assisted extraction—to gain information on their chemical composition. Parameters used to further monitor the modification process were dry matter, NPOC and UV-Vis analyses.

In addition, GC-MS was used to quantify low molecular weight compounds originating from the degradation of lignin during modification with ozone. Moreover, an attempt on the exploration of the oxidation mechanism was undertaken, based on the results from the GC-MS and a previously proposed degradation model by KUITUNEN ET AL. (2011).

3 Materials und Methods

3.1 Experimental methods

3.1.1 Materials

Indulin, a softwood Kraft lignin obtained from DKSH Holding Ltd. was used within this study as raw material. Its functional group content was determined by Dr. Ivan Sumerskii (Division of Chemistry of Renewable Resources), exhibiting 2.340 mmol/g of aliphatic hydroxyl groups, 3.680 mmol/g of aromatic hydroxyl groups and 0.422 mmol/g carboxyl groups.

The following substances were purchased from Sigma-Aldrich-Fluka-Merck (Sigma-Aldrich, Schnelldorf, Germany) and used without further purification: glyceric, malic, malonic, oxalic, and tartronic acid; sodium dihydrogen (NaH_2PO_4) and disodium hydrogen phosphate (Na_2HPO_4); sodium borohydride ($NaBH_4$); NaOH; ethanol (tech. grade); ethyl acetate (HPLC grade); anhydrous pyridine; methyl-α-D-galactopyranoside (MGP); o-ethylhydroxylamine hydrochloride (for GC); 4-(dimethylamino)-pyridine (purum) (DMAP); chlorotrimethylsilane (TMCS); and *N,O*-bis(trimethylsilyl)-triflouroacetamide (BSTFA). Hydrogen chloride (HCl) as 37% solution was purchased from VWR (VWR International, Vienna, Austria) and tartaric acid was purchased from Donau-Chemie (Donau Chemie AG, Wien).

The ^{13}C labeled glucose conversion product (^{13}C-GCP) was acquired from a previous project (LIFTINGER ET AL., 2015).

Amberlite XAD-7 (20-60 mesh)—a macroporous polyacrylate resin—and DOWEX 50WX8—a strongly acidic cation-exchange resin—were obtained from Sigma-Aldrich, but were prepared following the method by SUMERSKII, KORNTNER, ZINOVYEV, ROSENAU, & POTTHAST (2015).

Whatman Puradisc Aqua 30 / 0.45 CA filters were also purchased from Sigma-Aldrich.

3.1.2 Sample preparation

Lignin solutions were prepared by dissolving 40 g of the dry lignin powder in 360 g of a NaOH solution, leading to a concentration of 10% w/w. Using a set of three NaOH stock solutions varying in molarity (0.2, 0.4 and 1 M), three lignin solutions with different levels of pH, 10, 11 and 13 respectively, were achieved to study the effect of alkalinity on the modification process.

3.1.3 Modification procedure

The modification sequence was carried out in a small double-walled batch reactor with a capacity of 1 l, which was heated by a mixture of water and ethylene glycol to 80°C (Figure 15). The top of the reactor offered several inlets, which were used for attaching different equipment as described in the following. A long magnetic stirring rod mounted

on the lid was used for mixing and operated at 250 rpm. The required ozone/oxygen mix flow was supplied by a COM-AD-04 ozone generator from ANSEROS operating at
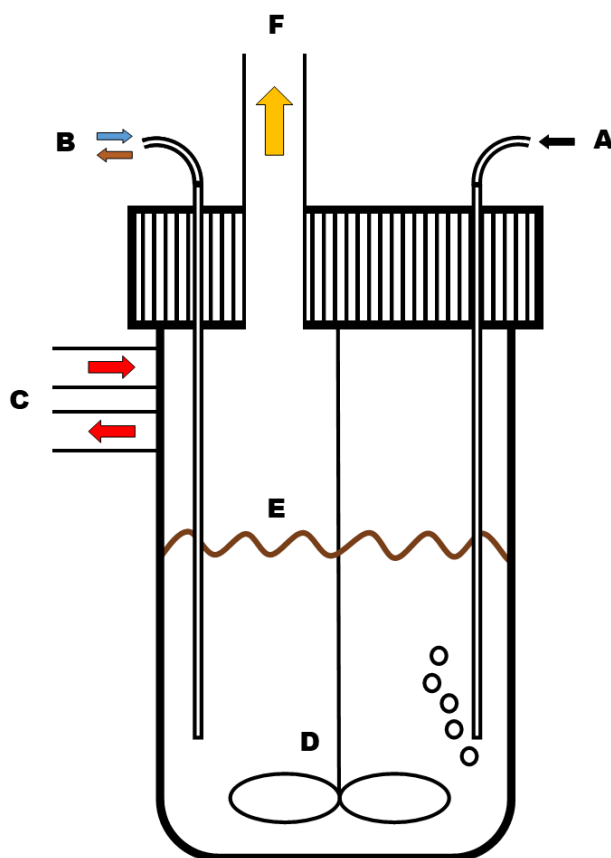

Figure 1: Schematic view of the used reactor: (A) ozone inlet (B) water inlet or sample outlet (C) heating system (D) stirring rod (E) filling level (F) exhaust

full capacity (100%) and providing a constant gas flow rate of 200 standard liters per hour, resulting in an ozone dosage of 17 g per hour. The stream was directly injected into the solution via a long stainless-steel capillary tube. Another capillary tube was either used to collect samples during reaction via an attached 15 ml glass syringe or to inject distilled water as a compensation for evaporating water (about 30 ml per hour), due to the elevated reaction temperature (80°C). One of the inlets was considered an outlet to maintain a safe and constant level of ambient pressure in the reactor and was connected to the vent via a long flexible tube. Additionally, a suction bottle was inserted between the reactor and the vent as a precautionary measure, because of the massive bubbling occurring in the beginning of the reaction. Besides preventing damage to the vent, it also offered a chance to quantify the loss of material due to the bubbling.

The oxidation reaction was carried out for a total of six hours, starting with the injection of the ozone/oxygen mix flow. Liquid samples of 10 ml were taken periodically (0, 20, 40, 60, 120, 180, 240, 300 and 360 minutes after the starting point) via the attached glass syringe and were therefore taken as a function of time. After sampling the capillary tube was flushed with distilled water for cleansing and for compensation of evaporated water.

3.1.4 Fractionation

In order to gain more information about the chemical composition of the samples, a two-step fractionation was performed (see Figure 16), leading to a total of five fractions for each sample available for analysis: crude (modified lignin), acid insoluble, acid soluble, adsorbed (aromatic) and non-adsorbed (non-aromatic).
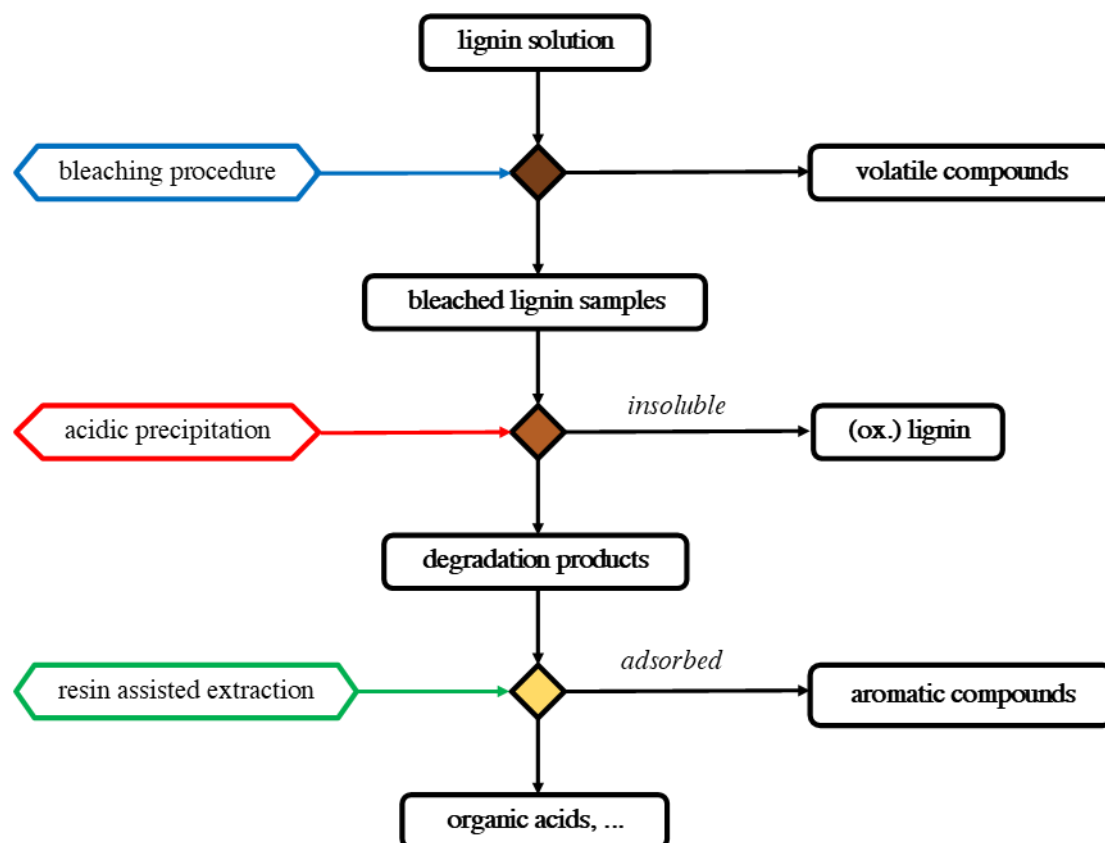

Figure 16: Schematic overview of the applied fractionation steps.

3.1.4.1 Acidic precipitation

For the first step of fractionation, a simple acidic precipitation was performed on 7 ml of the crude sample using a 1 M HCl solution to lower the pH level down to 1, allowing the acid insoluble part to divide from the soluble part present in the sample. Centrifugation was used to enhance the separation. Additionally, one washing step with a 1 M HCl solution was executed to further increase the purity of both, the insoluble and the soluble fraction.

3.1.4.2 Resin assisted extraction of aromatic compounds

A part of the acid soluble fraction was further undergoing an extraction step selectively separating aromatic compounds from non-aromatic ones. The micro scale approach as described by SUMERSKII ET AL. (2015) was deemed to be a proper method for this purpose and was therefore applied (Figure 17). A 10 ml syringe filled with 2 g of Amberlite XAD-7, and 1 g of DOWEX 50WX8 was used as extraction vessel for 4 ml

of the acid soluble sample fraction. Extraction took place over night at ambient temperature on a laboratory shaker.

Figure 17: Resin assisted extraction; micro scale approach by (SUMERSKII ET AL., 2015). Samples from the 1 M experiment; left (0 minutes) to right (360 minutes or bubbling loss). Dark color indicates solubilization of lignin fragments with increasing reaction time.

The non-adsorbed fraction was obtained by simply squeezing out the syringe after the extraction. Afterwards the resin was undergoing three washing steps with distilled water at pH 1 and three washing steps with usual deionized water to get rid of salts and other impurities. The desorption was carried out by four washing steps with ethanol (tech.) and one washing step with deionized water; providing the aromatic fraction.

3.2 Analytical methods

3.2.1 Dry matter analysis

Dry matter was determined of each fraction gravimetrically by drying 0.5 or 1 ml of the sample fraction in a drying oven at 105°C for 48 hours. In the case of the acid insoluble and the aromatic fraction, as they were not subjected to any other analysis, the whole sample fraction was dried and weighed.

3.2.2 Non-purgeable organic carbon analysis

This analysis was applied to the crude, acid soluble and non-adsorbed sample fractions. As a preparative step 2 ml of each fraction was diluted with 18 ml of the correspondent NaOH stock solution, 0.2, 0.4 and 1 M respectively. Subsequently, the diluted samples were filtered through Whatman Puradisc Aqua 30 / 0.45 CA filters. The measurement was performed on a Shimadzu TOC-VCPH with an ASI-V autosampler. Oxygen was used as carrier gas. The actual measurement was conducted by Ing. Marion Sumetzberger-Hasinger at the Institute of Environmental Biotechnology (IFA Tulln) of Boku University.

3.2.3 UV/Vis spectroscopy

The UV/Vis measurements were applied to the crude, acid soluble and non-adsorbed sample fractions. The measurements took place at a pH Level of 8 using a sodium hydride phosphate buffer solution for dilution, which also served as blank. The phosphate buffer solution was prepared using 20 ml of a 0.5 M NaH_2PO_4 solution, 380 ml of a 0.5 M Na_2HPO_4 solution and 600 ml of deionized water.

The measurements were performed on a LAMBDA 45 UV/Vis Systems instrument by Perkin Elmer (Waltham, MA) in the range between 200 and 800 nm.

Borohydride reduction was achieved by applying 10 mg of $NaBH_4$ as reducing agent to each sample after the primary UV/Vis measurement. The reaction time was about 24 hours. The excess of generated hydrogen was removed by shaking on a laboratory shaker for 10 minutes.

3.2.4 Gas chromatography and mass spectroscopy (GC-MS)

3.2.4.1 Standards

Calibration data was either retrieved from earlier experiments done by LIFTINGER ET AL. (2015), as in the case of glycolic acid, lactic acid, 3-hydroxypropanoic acid, glycerol and succinic acid, or was obtained by own measurements, which was done for oxalic acid, glyceric acid, malonic acid, tartronic acid, malic acid and tartaric acid. Calibration was done as a triple determination using standard samples with concentrations of 20, 40, 80, 120, 150 or 200 µg/µl, which were prepared from stock solutions with concentrations of 2 g/l. Subsequently, lyophilization was performed at -105°C for one day. MGP (internal standard II) was considered suitable for internal standardization and was introduced in the course of sample derivatization (see section 3.2.4.3 Derivatization: oximation and silylation below).

3.2.4.2 Samples

1 ml of the crude sample fraction of each sample was used for GC-MS analysis. The pH level was neutralized using either NaOH (1 or 3 M) or HCl (1 or 3 M), which caused precipitation in some of the samples. Centrifugation was applied to gather a particle free supernatant. From the supernatant 150 µl were transferred to a 4 ml vial, then 75 µl of the ^{13}C-GCP (internal standard I) was added. Subsequently, the sample-internal standard mixture was frozen at -80°C and lyophilized for one day.

3.2.4.3 Derivatization: oximation and silylation

The procedure was exactly carried out as described by LIFTINGER ET AL. (2015). For oximation, 200 µl of anhydrous pyridine containing 40 mg/ml o-ethylhydroxylamine hydrochloride and 1 mg/ml MGP (internal standard II) were added to the lyophilized sample, before the vial was closed and heated up to 70°C for one hour in an oven. Afterwards, 200 µl of anhydrous pyridine containing 1.5 mg/ml DMAP and 200 µl

BSTFA containing 10% TMCS were added for silylation, which was performed at 70°C for two hours. Shortly after the samples had cooled down to ambient temperature, 600 µl of ethyl acetate were added and a last centrifugation step was conducted. For injection into the GC-MS, an aliquot of 0.2 µl was taken from the supernatant.

3.2.4.4 GC MS analysis

Analysis was conducted on an Agilent 7890A gas chromatograph coupled with an Agilent 5975C triple axis mass selective detector (MSD; Agilent Technologies, Santa Clara, CA, USA). A non-polar DB5-MS column (30×0.25 mm i.d. × 0.25 µm film thickness) obtained from J&W Scientific (Folsom, CA, USA) was used. A CTC-PALxt autosampler was used for sample injection and was controlled by Chronos software v.3.5 (Axel Semrau, Spockhövel, Germany).

In general, operating conditions of the GC were simply chosen in accordance to Liftinger et al. (2015). Helium was used as carrier gas with a constant column flow of 0.9 ml/min. Splitless injection was applied with an injector temperature of 260°C (constant) and a purge flow of 15.0 ml/min for 0.75 minutes. The temperature gradient profile was as follows: 50°C for 2 minutes, followed by an increase by 5°C per minute to 280°C, then 280°C for 20 minutes. The mass selective detector was operated in EI-mode (70 eV ionization energy at 1.13×10^{-7} Pa) with an ion source temperature of 230°C. Temperature of the quadrupole and the transfer line were 150 and 280°C, respectively. Data were acquired in Scan mode ranging from 45 to 950 m/z.

The NIST/Wiley 2008 database was used for compound identification.

4 Results and Discussion

4.1 pH measurement

The pH of every sample set (0.2/0.4/1 M) was monitored (Figure 18), as the predominant oxidative reaction mechanism is mainly governed by the current pH value due to its strong influence on the decomposition of ozone into its various reactive species (BABLON ET AL., 1991; HORVÁTH ET AL., 1985).

The initial pH levels of the 0.2, 0.4 and 1 M experiments were 9.8, 11.3 and 13, respectively. The 0.2 and 0.4 M experiments showed a strikingly similar behavior with an initially rapid decrease to pH levels of 2.4 and 3 respectively, followed by a much slower decrease, resulting in final pH levels of 1.1 and 1.9 respectively. Although a rather steep decrease in pH could be expected from literature, the reduction was still more vigorous than most authors described (KALLIOLA ET AL., 2011, 2015; WANG ET AL., 2004). This may be owed to the high lignin concentration (10% w/w) in combination with the applied high ozone dosage of 17 g per hour, leading to a very intense oxidation process. However, the 1 M experiment experienced not only a much smoother change, but also a less severe reduction in pH level. After an initial delay, pH dropped promptly to 9.6, followed by a steady but attenuated decrease to a final pH of 4.7.
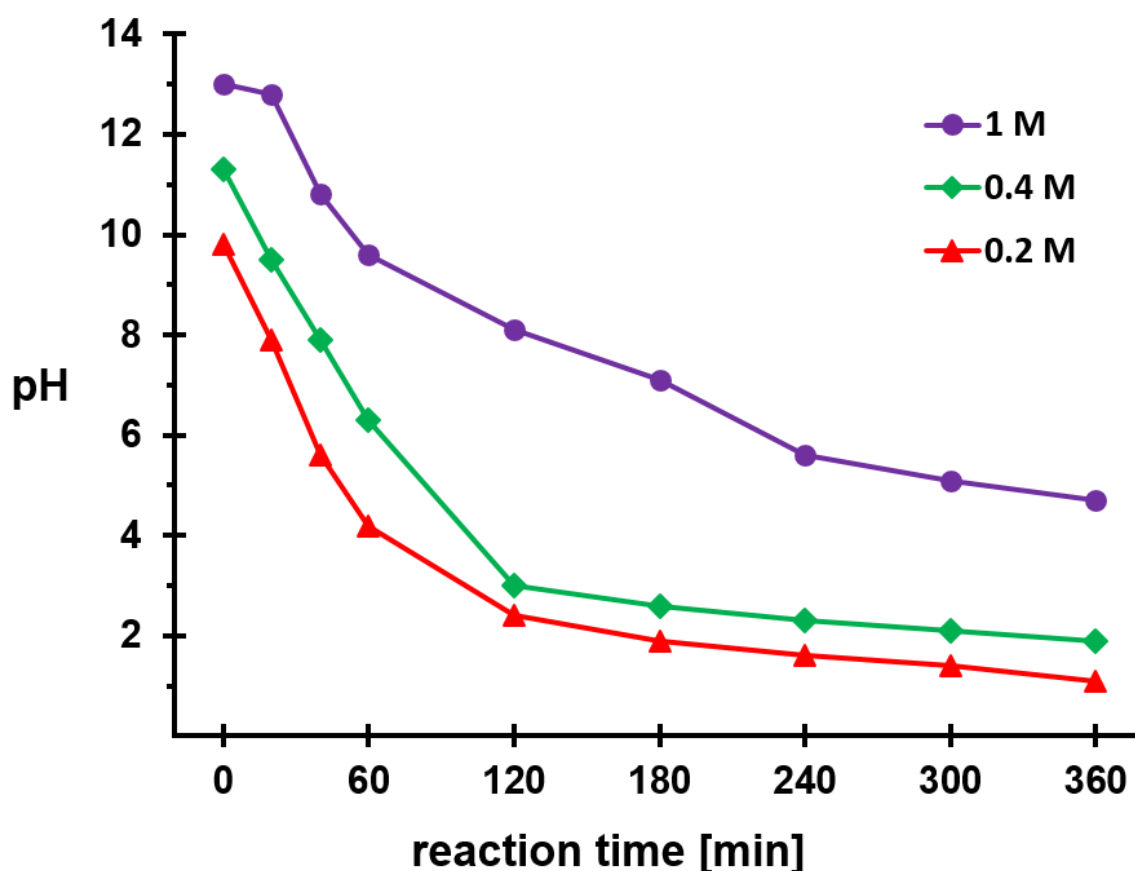
Figure 18: Change in pH over time. The 0.2 and 0.4 M experiments show a similar development in pH with an initially severe decrease. In contrast, the 1 M experiment shows a smoother decrease; only slightly below neutral.

Considering the changing composition of active species with pH, major differences in the oxidation process are indicated by the difference in the development of pH between the 0.2 or 0.4 M and the 1 M experiment. Only the initial oxidation of the 0.2 or 0.4 M experiment is influenced by the predominance of hydroperoxyl ($HO_2\bullet$) and hydroxyl radicals ($HO\bullet$), as the pH level is dropping rapidly below neutral within the first 60 minutes. The later progression is mainly related to molecular ozone (WANG ET AL., 2004). In contrast, the oxidation of the 1 M experiment is initially influenced by the predominance of superoxide radical ($O_2^-\bullet$) and hydroperoxide anions, before pH drops below 10 and hydroperoxyl ($HO_2\bullet$) and hydroxyl radicals ($HO\bullet$) become predominant (WANG ET AL., 2004). In the later phase, decomposition slows down with decreasing pH level and therefore molecular ozone is gaining influence in the oxidation process.

4.2 Fractionation

The fractionation yielded additional sample fractions (acid soluble or insoluble, adsorbed or non-adsorbed) to the original crude fraction (Figure 19, Figure 20, Figure 21 and Figure 22). In general, the crude fraction showed a clear reduction in color intensity with reaction time as well as a shift in color from black or brownish towards reddish or yellow. Since the 0.2 and 0.4 M experiments show a more pronounced reduction color intensity, degradation was presumably more vigorous compared to the 1 M experiment.
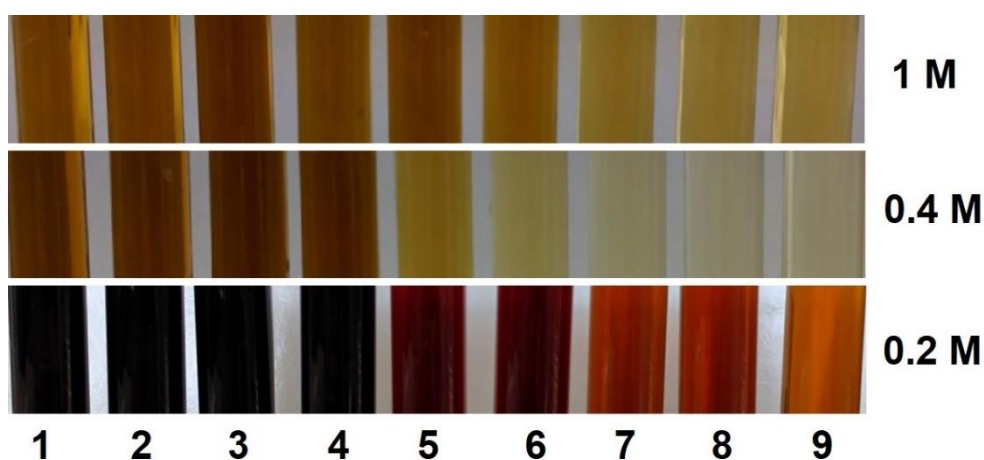
Figure 19: Crude sample fraction of the 0.2, 0.4 and 1 M experiment; left (0 minutes) to right (360 minutes). The 0.4 and 1 M experiment are shown with a higher dilution compared to the 0.2 M experiment. Color is changing from black (dark brown) to orange-red (yellow) and intensity is decreasing with increasing reaction time.

The acid soluble sample fraction showed increasing color with reaction time, indicating an intensive solubilization of compounds. The dark auburn color of the later samples of the 1 M experiment indicates a much more pronounced solubilization compared to the samples of the 0.2 and 0.4 M experiments.
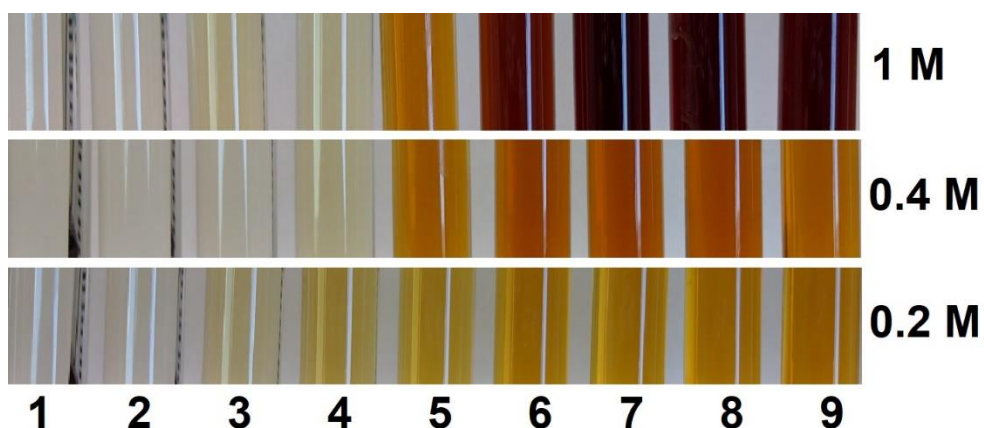
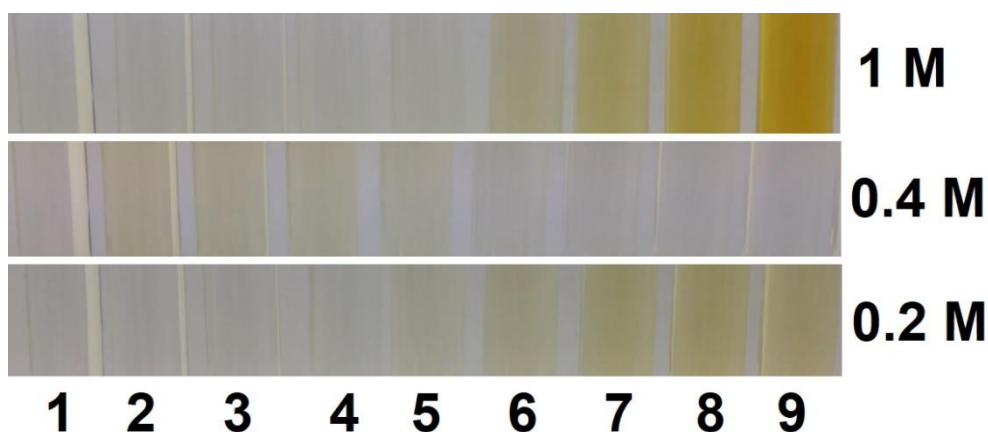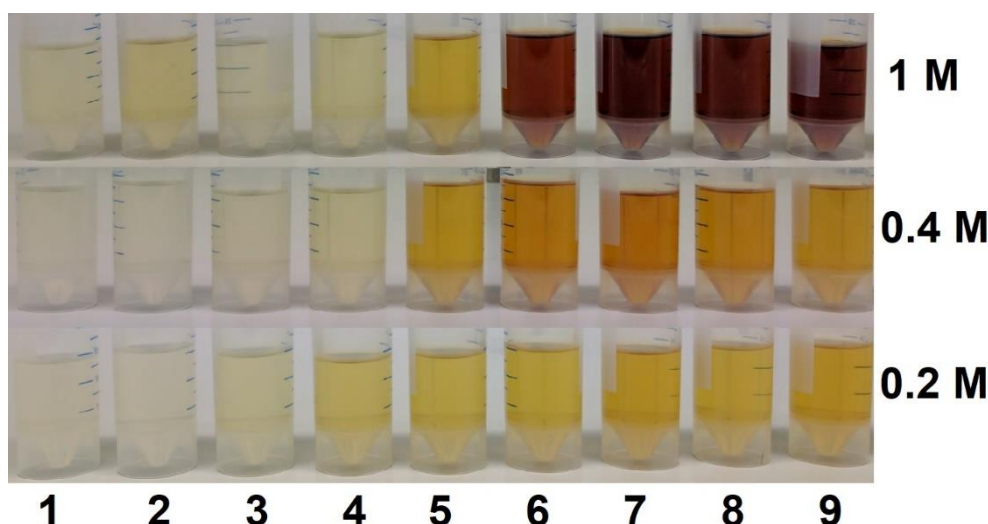**Figure 20: Acid soluble sample fraction of the 0.2, 0.4 and 1 M experiment; left (0 minutes) to right (360 minutes). Color is increasing with reaction time, indicating increasing solubilization.**

Overall, the non-adsorbed sample fraction showed very low color intensity as expected, only the later samples of the 1 M experiment—and to a lesser extent the later samples of the 0.2 M experiment—showed some color. Therefore, an insufficient resin assisted extraction was presumed, as the non-adsorbed (non-aromatic) compounds should not exhibit any color.

Figure 21: Non-adsorbed (non-aromatic) sample fraction of the 0.2, 0.4 and 1 M experiment; left (0 minutes) to right (360 minutes). Color is increasing with reaction time, indicating increasing solubilization. The 0.4 M experiment shows color only within the first 120 minutes.

The absorbed (aromatic) sample fraction showed a clear increase in color with reaction time, indicating solubilization of aromatic compounds to some degree within all experiments. However, the later samples of the 1 M experiment exhibit the strongest color, indicating a much more pronounced solubilization of aromatic compounds compared to the 0.2 and 0.4 M experiments.

Figure 22: Adsorbed (aromatic) sample fraction of the 0.2, 0.4 and 1 M experiment; left (0 minutes) to right (360 minutes). Color is increasing with reaction time, especially in the 1 M experiment, indicating increasing solubilization of aromatic compounds.

4.3 Gravimetric dry matter analyis

The gravimetric dry matter analysis was primarily applied to distinguish the degree of volatilization during the process. Additionally, sample fractionation yielded a partitioning of the non-volatile residuals to estimate the degree of solubilization. Dry masses were corrected by subtracting the estimated salt content. The content of sodium was estimated according to the filling level of the reactor at the time of sampling, while for chloride, the amount of applied hydrochloric acid in the acidic precipitation as well as the expected amount of sodium had influence on the estimation. Despite all the careful calculations, determination of the ash content would have resulted in better accuracy of the results, especially in case of the precipitated and extracted fractions, and is suggested for future experiments. Furthermore, intensive foaming, which usually occurred within the first 60 minutes, caused an undesired loss of material to some extent. Nevertheless, characteristic trends are reflected sufficiently accurate by the results of the 0.2, 0.4 and 1 M experiments (Figure 23). The 0.2 M experiment showed a steep linear decrease in total dry matter within the first 120 minutes down to 31% of the original weight, followed by a rather slow decrease. The 0.4 M experiment showed overall a quite similar trend, only with a slightly less steep initial decrease of the total dry matter. Therefore, both experiments exhibited vigorous degradation to volatile compounds as initially hydroxyl (HO•) and hydroperoxyl radicals (HO$_2$•) were dominating, but when pH dropped to approximately 2 and molecular ozone was the only predominant active species, the reduction of organic matter was limited to some extent. This observed behavior matches well with the experience gained from waste water ozonation trials (ALVARES ET AL., 2001; GOGATE & PANDIT, 2004), indicating analogies in the oxidation process. Interestingly, the 1 M experiment showed an entirely different trend. Here, transformation to non-volatile compounds was the dominating oxidation mechanism, as the decrease in total dry matter was much less severe, although fast reacting hydroxyl (HO•) and hydroperoxyl radicals (HO$_2$•)

were present for most of the reaction time. Apparently, the prevention of a severe drop of pH to neutral during the initial fast degradation of relatively easy oxidizable fractions, pose to be the explanation for this exceptional less pronounced volatilization. Hence, starting the oxidation at higher pH levels appear to be a promising approach to avoid intensive degradation of the lignin and rather promote oxidative modification.
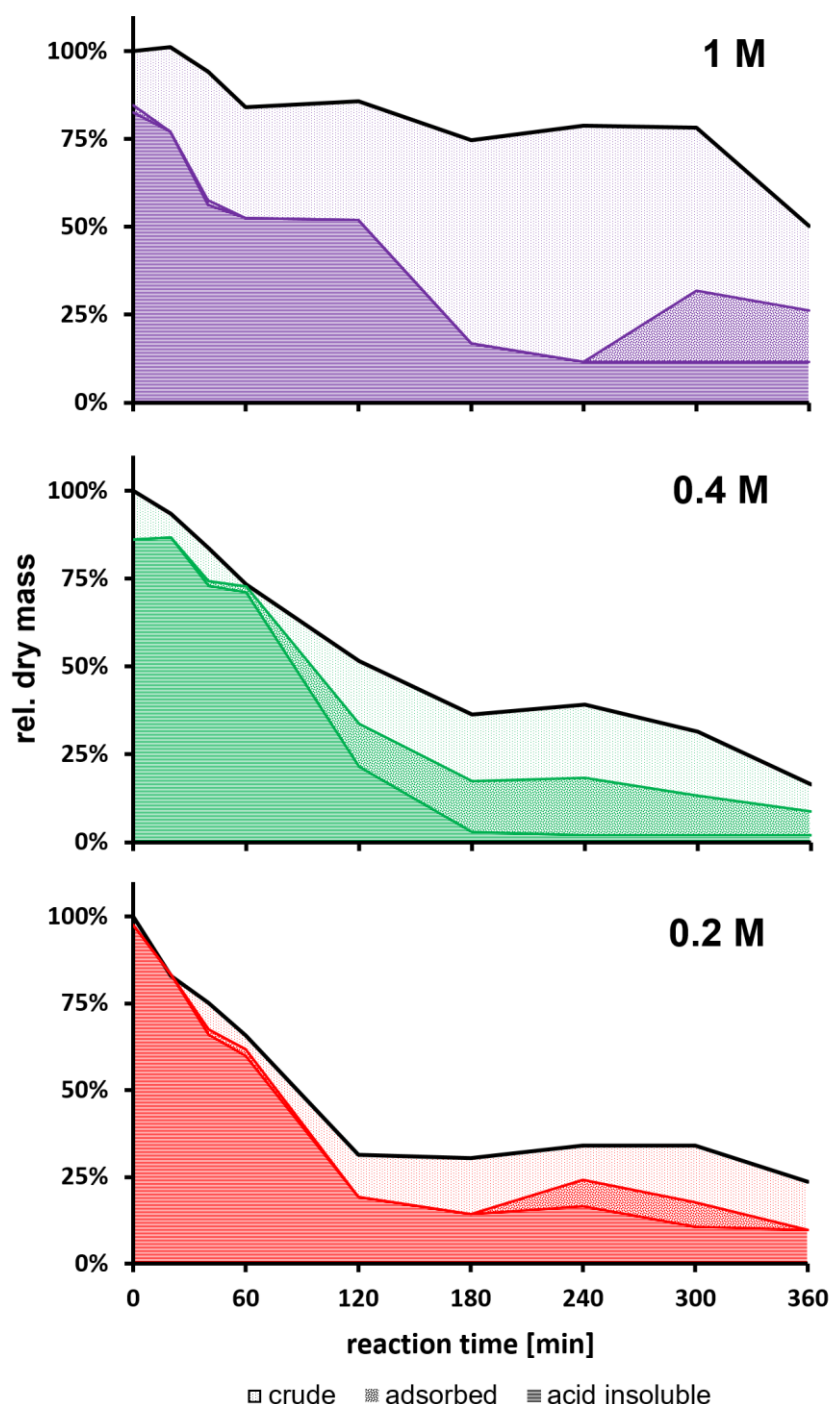

Figure 23: Development of the rel. dry mass over time. The 0.2 and 0.4 M experiments show a much higher loss in dry mass of the crude fraction compared to the 1 M experiment. All experiments show a solubilization of non-adsorbed (non-aromatic) as well as adsorbed (aromatic) compounds.

Some indications to verify this interpretation can be drawn from reviewing the results from the fractionation (Figure 23). As mentioned before, fractionation was carried out to achieve information on changes in solubility during the oxidation process. Basically, solubility is steadily increasing, as the lignin stays soluble throughout the entire process, despite a continually declining pH value. But precipitated lignin can still be found to some extent after the reaction, representing 5, 2 or 12% of the original dry matter in the 0.2, 0.4 and 1 M experiment, respectively. Since the harsh acidic precipitation at pH 1 results in a complete separation of a partly modified from a strongly oxidized fraction, the degree of transformation to non-volatile compounds of lower molecular weight can be roughly estimated. In addition, the results from the resin assisted extraction delivers some information on the proportion of aromatic compounds within the acid soluble fraction.

Regarding the 0.2 M experiment, the formation of an acid soluble fraction is only starting in the very late phase, when most of the original dry matter has already been converted to volatile compounds and molecular ozone has become the predominant active species. Still, up to 17% of the original dry matter is converted to acid soluble compounds, including aromatic compounds representing up to 7% of the original dry matter. Additionally, the residual insoluble fraction represents to a substantial extent the precipitated lignin found after the end of reaction, indicating the still soluble oxidized lignin has been completely converted by transformation to acid soluble compounds during the later phase of oxidation. In the 0.4 M experiment, transformation to acid soluble compounds has been found to occur earlier compared to the 0.2 M experiment, even alongside volatilization. The proportion of the acid soluble fraction was also found to be higher, up to 33% of the original dry matter. Furthermore, the proportion of aromatic compounds was also much higher, representing up to 16% of the original dry matter. Most likely, as smaller amounts of precipitated lignin were found after the end of reaction, much more oxidized lignin was still soluble and therefore available for transformation. As the much lower decrease in total dry matter is already indicating, the 1 M experiment is much more characterized by transformation to acid soluble compounds than by volatilization. However, up to 17% of the original dry matter was found to be acid soluble right from the start of the reaction. Nonetheless, the acid soluble fraction is increasing slowly in the beginning, followed by a steep increase from 34 to 58% of the original dry matter within just one hour. The proportion of aromatic compounds have also been found to be somewhat higher, representing up to 20% of the original dry matter. Similar to the 0.2 M experiment, a considerate amount of precipitated lignin was found in the 1 M experiment after the reaction. But in the later case, it is much more difficult to estimate when the lignin has precipitated, as there is not such a rapid drop below neutral. Anyways, it can also be presumed that the still soluble oxidized lignin has been completely transformed to acid soluble compounds in the later phase of oxidation, as not much insoluble dry matter was found in the liquid samples after 180 minutes of reaction.
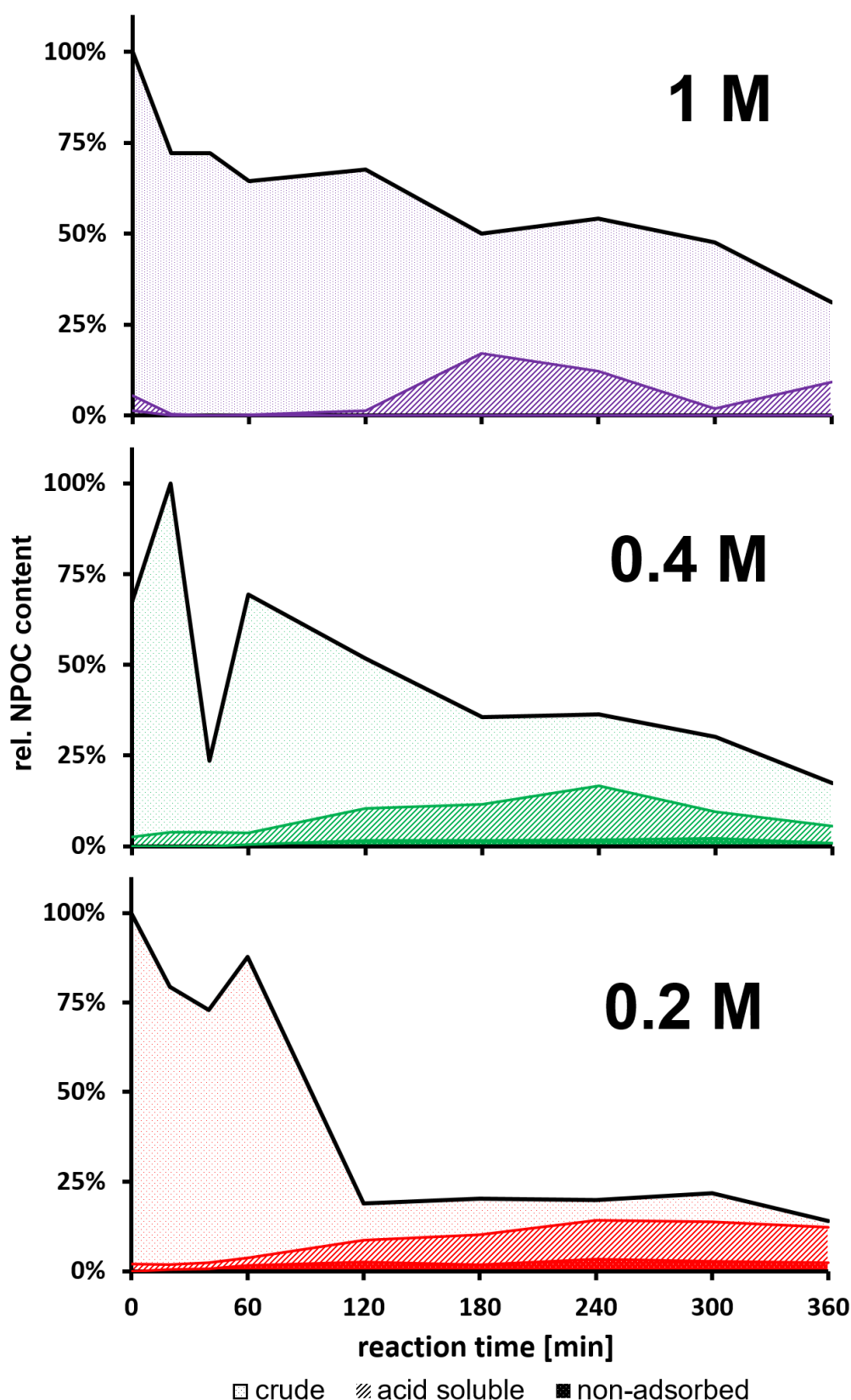
Figure 24: Development of NPOC over time. The 0.2 and 0.4 M experiments show a more severe loss in NPOC of the crude fraction than the 1 M experiment. Acid soluble NPOC rises up to 17% of the original NPOC, indicating steady solubilization in all experiments. Non-adsorbed NPOC was only observed in the 0.2 and 0.4 M experiments, however, only up to 3% of the the original NPOC.

4.4 Non-purgeable organic carbon analysis

NPOC was determined to overcome the distortion of the gravimetric determination due to the massive introduction of oxygen and the potentially inaccurate estimation of the salt content.

All in all, the NPOC results are in good agreement with the results from the gravimetric determination for all experiments (Figure 24). Therefore, conclusions drawn from the dry matter determination apply to the NPOC measurement as well. Interestingly, the NPOC of the crude fraction is steadily decreasing, revealing that volatilization is occurring at different degrees among all experiments throughout the entire process (Figure 24). The loss in NPOC of the crude fraction accounts for 86, 83 or 69% of the original NPOC of the 0.2, 0.4 and 1 M experiment, respectively. Compared to KALLIOLA ET AL. (2011), removal of organic carbon was much more pronounced, easily exceeding the reported 10 – 20% (in 240 minutes). This is certainly related to the much lower ozone dosage applied by KALLIOLA ET AL. (2011).

Solubilization is usually starting after 60 minutes and is clearly displayed as a steady increase of carbon in the acid soluble fraction up to 17% of the original carbon content (Figure 24). The same applies to the non-adsorbed fraction, which makes up to 3% of the original carbon content, except for the 1 M experiment as the blank value was higher than the measured values.

4.5 UV Vis measurement

The UV Vis measurement was performed to track the content of either aromatic (at 280 nm) or chromophoric (quinoid; at 457 nm) structures. Results are displayed in Figure 25 for 280 nm and Figure 26 for 457 nm, including the results from borohydride reduction. The absorbance of the crude fraction (0 minutes) was believed to represent the initial content and was therefore set to 100%.

4.5.1 Aromatic content

The 0.2 and 0.4 M experiments showed a rapid decrease in absorbance within the first 180 minutes and a low, if any, aromatic content left at the end of the reaction. However, absorbance within the acid soluble fraction is clearly rising after 60 minutes, indicating a solubilization of compounds containing aromatic moieties. The reason why the absorbance of the acid soluble fraction is exceeding the absorbance of the crude fraction remains unknown. Therefore, a quantitative comparison between the fractions seemed not to be reliable. In the samples of the non-adsorbed fraction, no aromatic content was detected, hence the complete extraction of aromatics was successful in both experiments. In the 1 M experiment, absorbance at 280 increased within the first 120 minutes, followed by a less rapid decrease, resulting in comparably higher amounts of residual aromatics still present after 360 minutes. Moreover, the aromatic content also appears to be considerably higher in the acid soluble fraction compared to the 0.2 or 0.4 M experiment, indicating a much more pronounced solubilization of

compounds containing aromatic moieties in the 1 M experiment. Although the absorbance of the acid soluble fraction is not exceeding the absorbance of the crude fraction, quantitative comparison between the fractions was omitted, since absorbance could still be overestimated, as in the case of the other experiments. Unfortunately, aromatic content was observed in the later samples of the non-adsorbed fraction, indicating an insufficient extraction of aromatics.
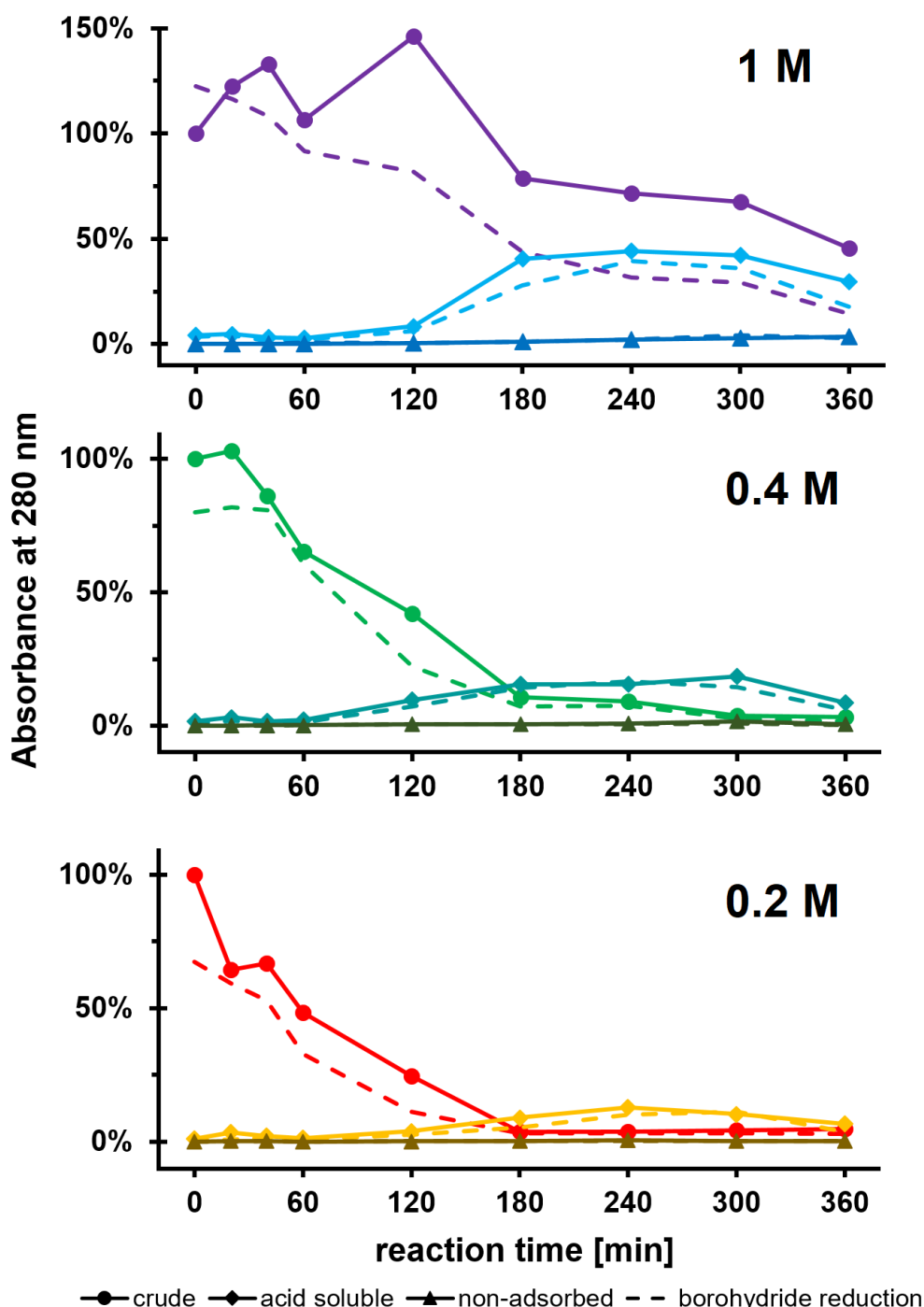

Figure 25: Results of the UV-Vis measurement at 280 nm. The 1 M experiment exhibited a less pronounced decrease in aromatic content. After 60 minutes, aromatic content is increasing in the acid soluble fraction among all experiments. Insufficient extraction of aromatics is indicated by absorbance in the non-adsorbed fraction of the 1 M experiment.
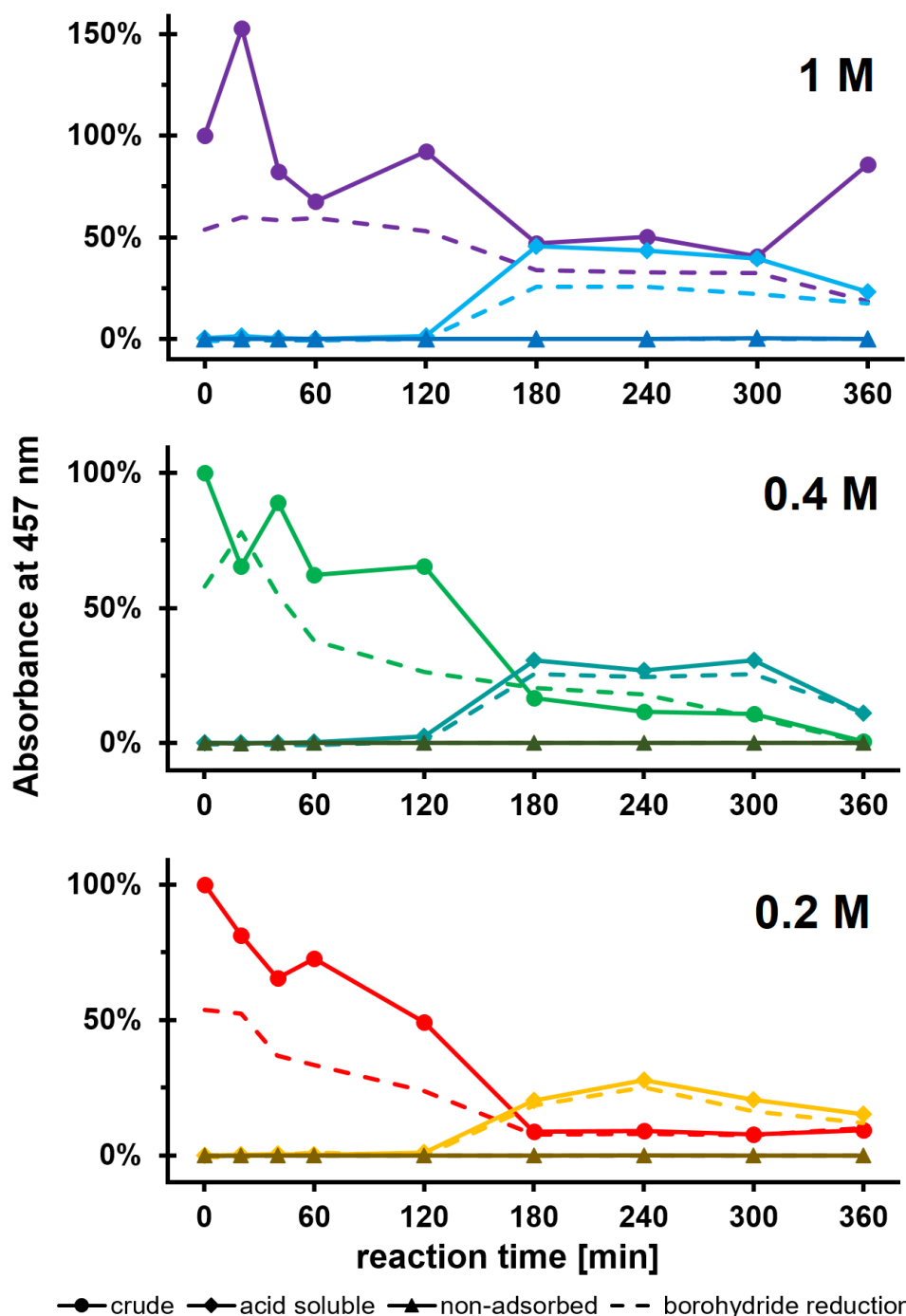
Figure 26: Results of the UV-Vis measurement at 457 nm. Chromophoric content is decreasing within the first 180 minutes among all experiments. The 1 M experiment exhibited a smoother and less severe decrease. After 120 minutes, the chromophoric content is increasing in the acid soluble fraction among all experiments. The non-adsorbed fraction did not show any absorbance.

4.5.2 Chromophoric content

In general, absorbance at 457 nm was initially about 20% of the absorbance at 280 nm among all experiments. Since no absorbance was observed in samples of the non-adsorbed fraction, absorbance at 457 nm was presumed to be exclusively linked to derivatives of aromatic compounds.

Concerning the 0.2 or 0.4 M experiment, chromophoric structures suffer severe degradation within the first 180 minutes, as in the case of aromatic moieties. Moreover, chromophoric content is significantly increasing in the acid soluble fraction after the first 120 minutes. Again, the reason why the absorbance of the acid soluble fraction is exceeding the absorbance of the crude fraction remains unclear. Therefore, quantitative comparisons between the fractions were again omitted. The 1 M experiment exhibits not only a smoother, but also less severe reduction in the chromophoric content with a much higher amount of residual chromophoric compounds. Furthermore, solubilization of chromophoric content is occurring to an even greater extent after 120 minutes, compared of the other experiments. Quantitative comparison between the fractions was also omitted, as absorbance could be overestimated as well.

4.5.2.1 Borohydride reduction

Concerning samples of the crude fraction, borohydride reduction always resulted in a reduced absorbance at 280 nm after the treatment throughout all experiments. This lacks a conclusive explanation, as according to GOLDSCHMID (1971), aromatic content should rather increase due to the treatment. In contrast, the aromatic content of the acid soluble fraction exhibited either no significant change (0.2 or 0.4 M) or also a reduction (1 M) after the treatment. Considering the experienced lowering in the aromatic content after the treatment in samples of the crude fraction, it remains rather unclear, whether a reduction of quinoid structures and thus an increase in the aromatic content have or have not really occurred. The same difficulties are faced reviewing the results at 457 nm. Although borohydride treatment led to the expected reduction in absorbance, it is still not clear whether it is solely based on the reduction of chromophoric structures or exposes errors in the measurement, as samples of the crude and the acid soluble fraction behave so differently.

4.6 Gas chromatography & mass spectroscopy (GC-MS)

4.6.1 Calibration

Calibration was carried out for oxalic, malonic, malic, glyceric, tartronic and tartaric acid, using MGP (internal standard II) as internal standard. In Figure 27, sample concentration is plotted against the averaged rel. response value. The results were fitted with a 2nd-degree polynomial fit forced through the origin. Coefficients of determination are displayed in Figure 27, ranging from 0.942 (tartronic acid) to 0.9976 (malic acid). As the fit indicates, malonic acid may be overestimated below and underestimated above 100 µg/ml to some extent.
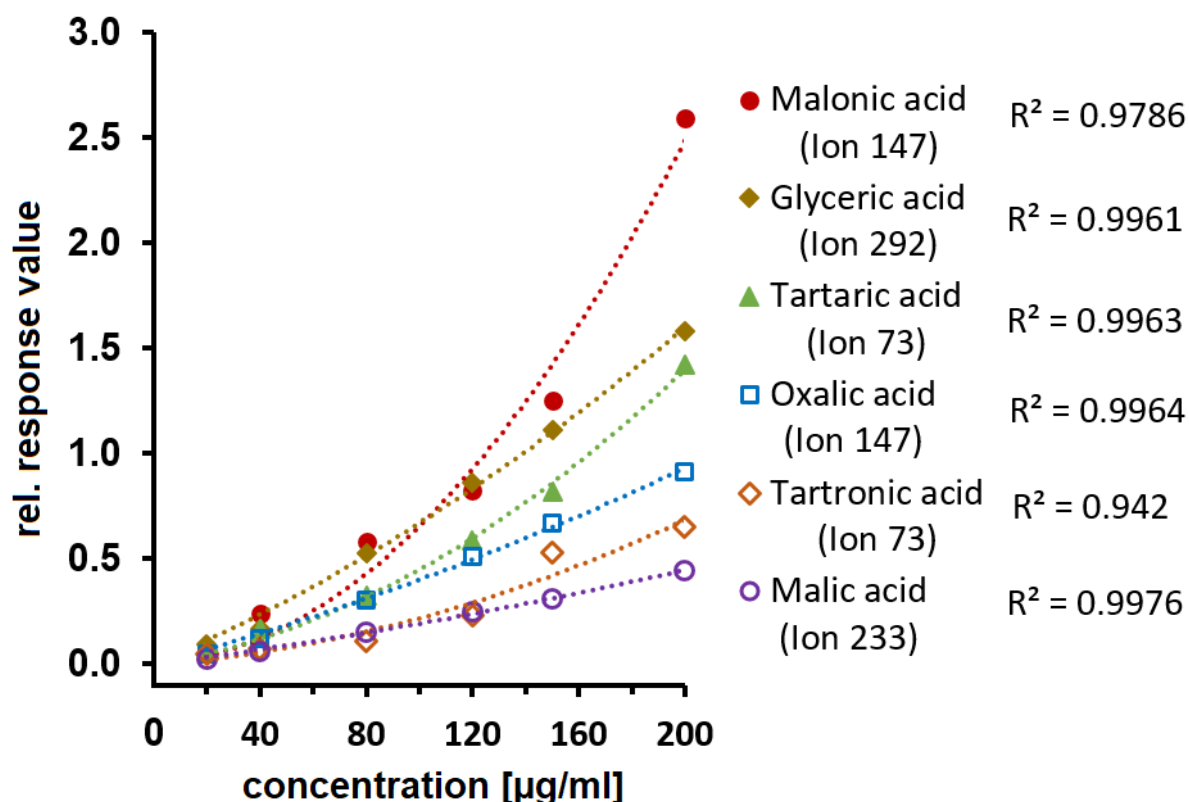
Figure 27: Results from the GC-MS calibration for several organic acids. The associated coefficients of correlation are displayed right next to the organic acids.

[13]C-labeled lactic acid originating from the ^{13}C glucose conversion product (internal standard I) was used as internal standard for lactic, glycolic, 3-hydroxypropanoic and succinic acid and glycerol. For these compounds, calibration data was retrieved from earlier experiments done by LIFTINGER ET AL. (2015). In addition, correct identification of the presumably assigned peaks was verified by authentic samples.

An overview on the analytes is given in Table 2, citing the retention time of the compound, the related internal standard and the selected target ion, which ensured the most accurate signal deconvolution.

Table 2: Internal standardization of the ozone oxidation analytes

RT [min]	IS	Analyte	Target ion [m/z]
10.7	I	13C Lactic acid	222
10.7		Lactic acid	219
11.1		Glycolic acid	205
14.2		3-Hydroxypropanoic acid	177
17.8		Succinic acid	247
18.1		Glycerol	147

Table 2 (continued)

RT [min]	IS	Analyte	Target ion [m/z]
30.1	II	MGP	204
12.9		Oxalic acid	147
14.9		Malonic acid	147
18.4		Glyceric acid	292
20.1		Tartronic acid	73
22.4		Malic acid	233
26.2		Tartaric acid	73

4.6.2 Non-volatile organic acid content

In Figure 28, the results from the GC-MS quantification of various organic acids and glycerol are shown for all experiments (0.2, 0.4 and 1 M). The calculation of the absolute weight values takes both dilution by neutralization and reactor filling level into account. Furthermore, the displayed weight values are given as carbon content, to exclude distortion by introduced oxygen and thus allow more accurate estimations on the transformation rate of lignin into organic acids.

The maximum organic acid content of the 0.2, 0.4 and 1 M experiments amounts 57.3, 79.0 and 104.0 mg carbon respectively, accounting for 0.2 to 0.4% of the original NPOC. In comparison, ROVIO ET AL. (2011) determined the content of non-carboxylic acids by capillary electrophoresis to be approximately 2.4 to 3.9% of the original TOC. However, regarding the acid soluble NPOC, the determined proportion of organic acids ranges from 1 to 2% for the 0.2 M and a bit higher to 4% for the 0.4 M experiment. The 1 M experiment revealed much higher variance in the acid soluble NPOC, therefore proportions are widely ranging from 2 to 100%. Hence, the actual proportions should be prudently estimated, probably ranging up to somewhat higher than 6% of the acid soluble NPOC. Interestingly, the organic acid content makes only up to 4 to 8% of the non-adsorbed NPOC for the 0.2 M and up to 15 to 27% for the 0.4 M experiment. As the results for the 1 M non-adsorbed NPOC were below the reference value of the blank, proportions can only be roughly estimated, but may be somewhat higher than the 0.4 M experiment, about 35% of the non-adsorbed NPOC. As the determined non-volatile organic acid content is only accounting for the minor portion of the acid soluble NPOC as well as the non-adsorbed NPOC, the mixture of degradation products from the oxidation process appears to be rather complex and diverse, demanding for a much more extensive investigation.
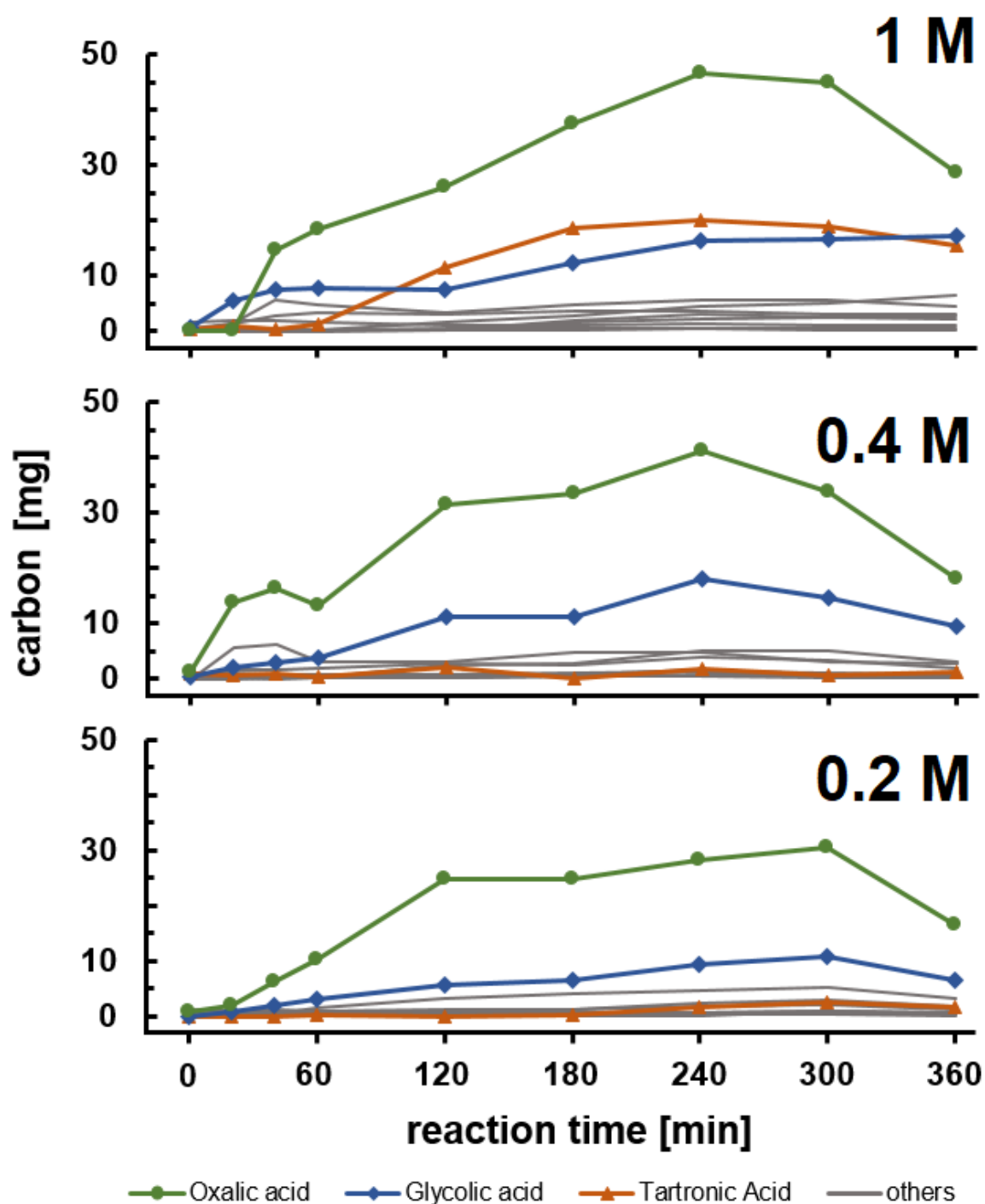
Figure 28: Formation of non-volatile organic acids during ozone oxidation of lignin. The predominant acids were oxalic and glycolic acid. In the 1 M experiment, tartronic acid showed a strikingly increased formation. Other acids were only formed in minor amounts (<5 mg).

Essentially, the obtained distribution of carboxylic acids appears to be in very good agreement with the results reported by ROVIO ET AL. (2011) (Figure 29). As it is clear from the results, oxalic acid and to a lesser extent glycolic acid, and tartronic acid in the case of the 1 M experiment, are the most common organic acids derived from the applied ozone oxidation process. Together, these acids account for more than 75% of

the organic acid content, whereby oxalic acid alone representing around 50% of the organic acid content. Moreover, oxalic acid shows a rapidly increase right from the start of the reaction, whereas glycolic or tartronic acid exhibit a much smoother increase over time. On the contrary, the formation of other organic acids and glycerol is far less pronounced, resulting in maximum amounts hardly more than 5 mg. Strikingly, the organic acid content, namely the content of oxalic and glycolic acid, is decreasing after hitting its maximum after 300 minutes for the 0.2 M and 240 minutes for the 0.4 and 1 M experiments. This was not expected from literature, as the reaction rates of organic acids with ozone are much lower compared to less oxidized compounds and therefore their content should at least remain rather stable (HOIGNÉ & BADER, 1983B). For one thing, neutralization during sample preparation for GC measurement may have an influence on the measured value. On the other hand, the decrease in organic acid content is amplified by including the filling level of the reactor into the calculation, indicating a possibly inaccurate determination of the filling level in the later phase of oxidation.
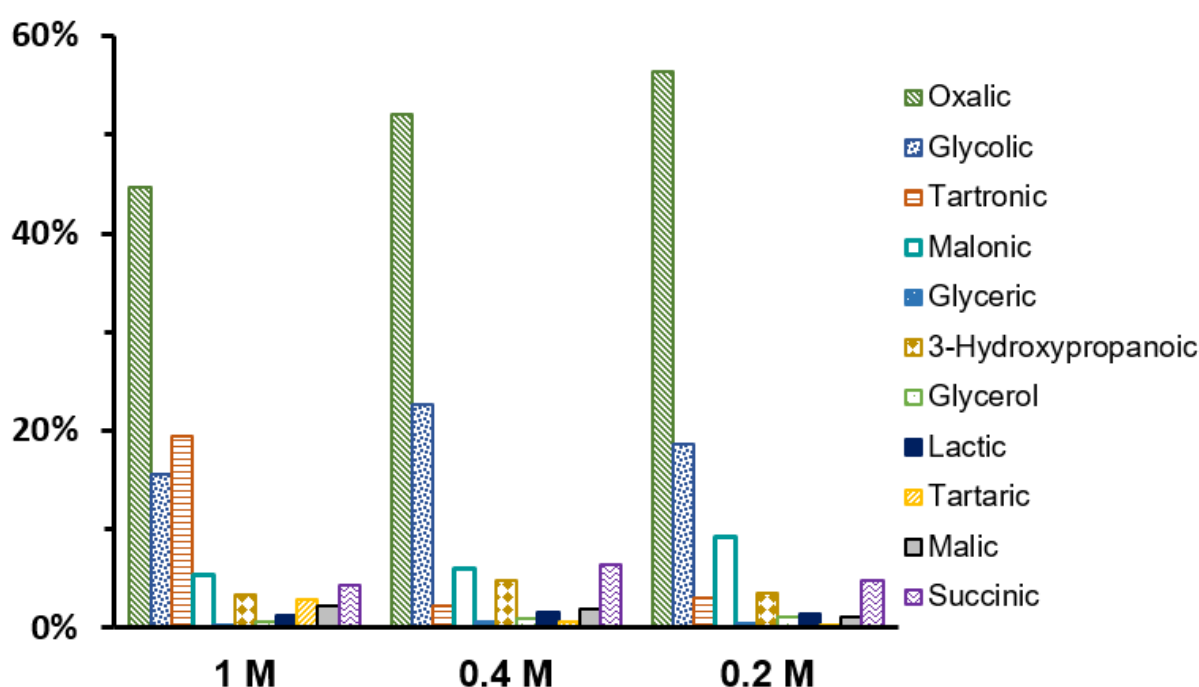
Figure 29: Proportions of the individual compounds after a reaction time of 240 minutes. Oxalic acid is clearly dominating, followed by glycolic and tartronic acid (1 M experiment).

4.7 Exploration of the ozone oxidation mechanism

According to the proposed degradation model by KUITUNEN ET AL. (2011), the various acids were clustered to represent specific reaction pathways, allowing a deeper insight into the oxidation mechanism. The clusters are divided into reactions involving either the aromatic ring or the aliphatic side chain. Additionally, sub-clusters were formed to differ certain types of ring-opening reactions (muconic acid or oxirane type) or sidechain cleavage (glycolic or glyceric type) from each other. Furthermore, acids

deriving from maleic acid were compiled in a separate subcluster, as they represent products from the further oxidation of hydroquinone derivatives deriving from glyceric type side chain cleavage (KUITUNEN ET AL., 2011). The assignment of the quantified compounds to the clusters is shown in Table 3.

Table 3: Assignment of compounds to clusters according to their origin in the oxidative degradation of lignin (model by KUITUNEN ET AL., 2011)

Cluster	Subcluster	Compounds	Degradation pathway
ring-opening	Muconic acid type	Oxalic acid	
	Oxirane type	Tartronic acid Malonic acid	
Side chain cleavage	Glycolic type	Glycolic acid	
	Glyceric type	Glyceric acid Glycerol 3-Hydroxypropanoic acid Lactic acid	
	Hydroquinone type	Tartaric acid Malic acid Succinic acid	

The results of the clustering are displayed in Figure 30 for all experiments. The cluster values are representing the amount of converted carbon expressed in mole, to enable

a comparison between the degradation pathways based on their frequency of occurrence. Overall, the proposed dominance of ring-opening reactions was clearly experienced, as they account for 60 to 80% of the recovered carbon. Moreover, degradation via the muconic acid pathway was predominant over the oxirane pathway, representing 85 to 90% of the ring-opening reactions. Interestingly, in the 1 M experiment, the oxirane pathway was more pronounced, accounting on average for 26% of the ring-opening reactions. Side chain cleavage was found to be accounting on average for about 27% of the recovered carbon, which is in good agreement with the results reported by ROVIO ET AL. (2011). Here, elimination of glycolic acid was occurring more frequently than elimination of glyceric acid derivatives at the ratio of 70 : 30 up to 85 : 15 with increasing reaction time. The hydroquinone cluster represents up to 6% of the recovered carbon in the 0.2 or 0.4 M experiment, and up to 8% in the 1 M experiment. When compared to the glyceric type cluster, in the later phase of oxidation the content of hydroquinone degradation products exceeds the predicted value from the glyceric type side chain cleavage by 70% for the 1 M experiment. Obviously, here, a degradation pathway besides the glyceric type is contributing to the formation of maleic acid derivatives. According to KUITUNEN ET AL. (2011), the degradation of conjugated phenols, i.e. enol ether structures, also yields in hydroquinone derivatives via vanillin intermediates. Therefore, quantification of vanillin (derivatives) is suggested for further investigations, as it would render further insight in the prevalence of certain oxidation pathways.

From the content of recovered organic acids, the amounts of volatile compounds can be estimated with this degradation model. Primarily, ring-opening reactions are proposed to be the main source for volatile compounds such as methanol, formic acid or carbonate (CO_3^{2-}), mostly by the degradation of muconic acid structures, whereas side chain cleavage renders only small contributions (KUITUNEN ET AL., 2011). According to the model by KUITUNEN ET AL. (2011), the amount of volatile compounds is exceeding the non-volatile organic acid content by at least five times. This rule applied on the results of the GC-MS quantification, the loss in NPOC due to volatilization is expected to be 1 to 2% of the original NPOC in the crude fraction. The proposed degradation model appears to be inadequate for the prediction of volatilization in ozone oxidation of lignin, as the observed loss in NPOC easily exceeds the expected value by far. Strikingly, the oxidation model by KUITUNEN ET AL. (2011) is underestimating degradation pathways, causing volatilization without the formation of non-volatile carboxylic acids. Therefore, future work in this field should attempt to implement these more accurately in degradation models, as they occur in a considerable frequency in the ozone oxidation process.
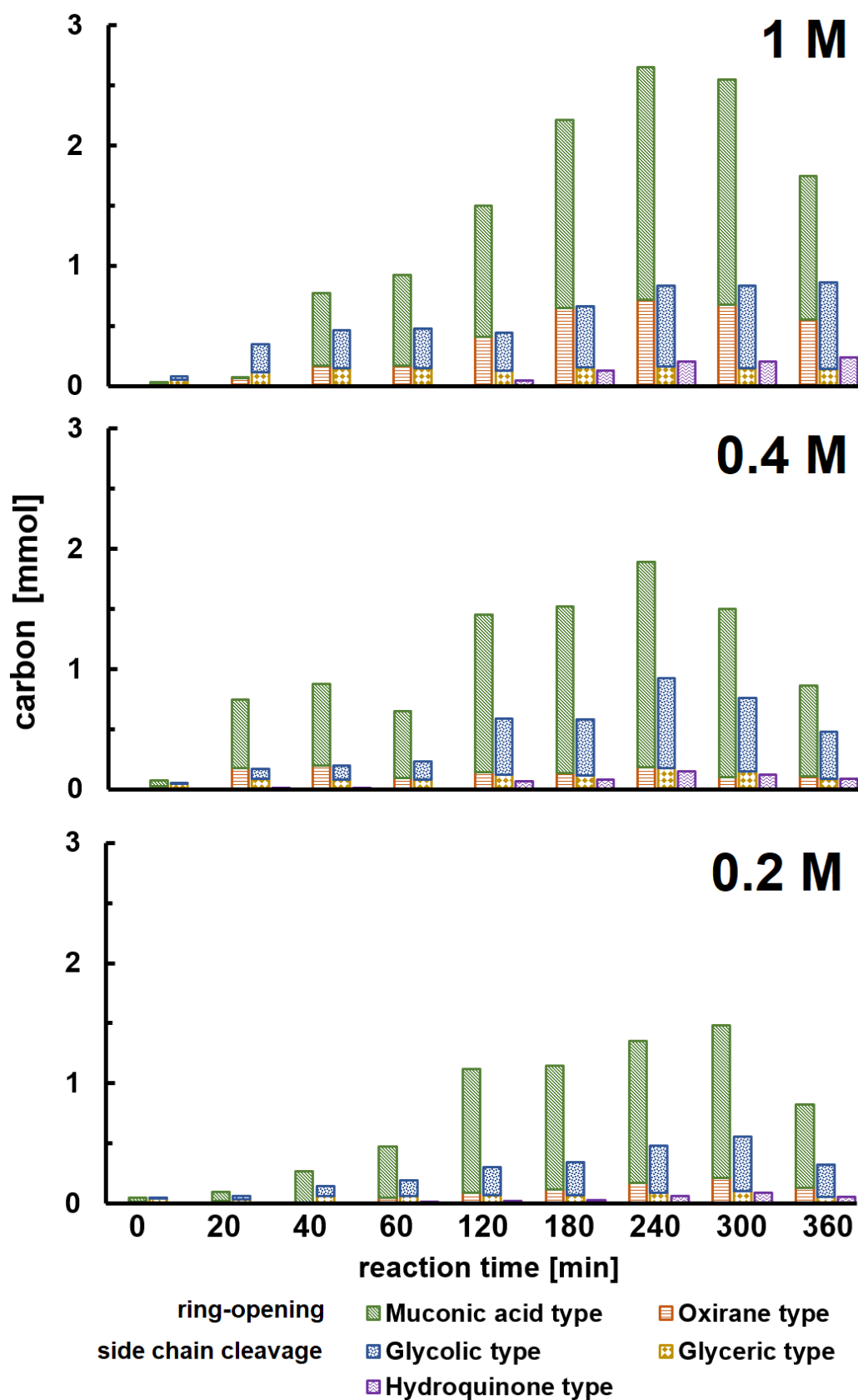
Figure 30: Clustered results from GC-MS quantification of non-volatile acids and glycerol over time. Ring-opening reactions of the muconic acid type are clearly dominating. In the case of side chain cleavage, reactions of the glycolic type occurred much more often than of the glyceric type.

5 Conclusion

Summing up, modification of Kraft lignin with ozone is strongly influenced by alkalinity, as modification at high alkalinity (1 M) resulted in different lignin properties compared to lower alkalinity (0.2 or 0.4 M).

The initial pH was found to be determining the predominance of either volatilization or transformation of lignin, as the 1 M experiment showed a much smoother and less severe decrease in total dry matter and NPOC compared to the 0.2 or 0.4 M experiment. Moreover, initial pH appeared to be more important with respect to the degree of volatilization than the mere presence of certain active species. Therefore, the prevention of a severe drop of pH during the initially fast degradation poses to be a promising approach to avoid intensive degradation of the lignin and rather promote oxidative modification. Nonetheless, volatilization of lignin steadily occurs throughout the entire process among all experiments, as the results from the NPOC determination showed a steady decrease in carbon.

Reviewing the results gained from analyses on the acid soluble and adsorbed fractions, solubilization processes were usually intensifying after an initial delay of 120 minutes and were characteristic for the later phase of the experiments. Besides a less pronounced volatilization, modification at higher alkalinity (1 M) exhibited also a less severe degradation of aromatic moieties, promoting rather their solubilization, as the results from the dry matter analysis and the UV-Vis measurement are indicating.

The quantification of degradation products via GC-MS yielded only in a low recovery of the original NPOC of the samples (0.2–0.4%), but the obtained distribution of several non-volatile compounds fits well with the reports from literature (ROVIO ET AL., 2011). Overall, oxalic acid was predominant by far, only followed by glycolic acid and—in the case of high alkalinity (1 M)—tartronic acid. Other organic compounds were found just in minor amounts.

Clustering the obtained results from GC-MS—according to the degradation model proposed by KUITUNEN ET AL. (2011)—allowed a deeper insight into the occurred oxidation process. Based on the clustering, the proposed predominance of ring-opening reactions over side chain cleavage could be confirmed. Reviewing the results from the subclustering, higher alkinity (1 M) led to a less frequent formation of muconic acid structures, instead promoting the oxirane degradation pathway to a certain degree. However, volatilization was heavily underestimated by the proposed model. Therefore, investigations focused on the volatile fraction are suggested for future projects, as they could be of help to improve already existing degradation models.

6 List of Figures

7 List of Tables

8 References

ALVARES, A. B., DIAPER, C., & PARSONS, S. A. (2001). Partial oxidation by ozone to remove recalcitrance from wastewaters--a review. *Environmental Technology*, *22*(November 2013), 409–427. https://doi.org/10.1080/09593332208618273

BABLON, G., BELLAMY, W., BOURBIGOT, M., DANIEL, B., DORÉ, M., ERB, F., … VENTRESQUE, C. (1991). Fundamental Aspects. In B. Langlais, D. Reckhow, & D. Brink (Eds.), *Ozone in water treatment – Application and engineering* (pp. 11–133). Chelsea, MI: Lewis Publishers, Inc.

BELTRAN-HEREDIA, J., TORREGROSA, J., DOMINGUEZ, J. R., & PERES, J. A. (2001). Kinetics of the reaction between ozone and phenolic acids present in agro-industrial wastewaters. *Water Research*, *35*(4), 1077–1085. https://doi.org/10.1016/S0043-1354(00)00343-2

BIERMANN, C. (1996). *Handbook of Pulping and Papermaking* (Second). San Diego, CA: Academic Press.

BIJAN, L., & MOHSENI, M. (2005). Integrated ozone and biotreatment of pulp mill effluent and changes in biodegradability and molecular weight distribution of organic compounds. *Water Research*, *39*(16), 3763–3772. https://doi.org/10.1016/j.watres.2005.07.018

BOERJAN, W., RALPH, J., & BAUCHER, M. (2003). Lignin Biosynthesis. *Annual Review of Plant Biology*, *54*(1), 519–546. https://doi.org/10.1146/annurev.arplant.54.031902.134938

BRÄNNVALL, E. (2009). Overview of pulp and paper processes. In M. Ek, G. Gellerstedt, & G. Henriksson (Eds.), *Pulp and paper chemistry and technology Vol. 2* (pp. 1–13). Berlin, GER: Walter de Gruyter, GmbH & Co KG.

BRUNOW, G. (2005). Methods to Reveal the Structure of Lignin. *Lignin, Humic Substances and Coal*, 89–99. https://doi.org/10.1002/3527600035.bpol1003

BRUNOW, G., & LUNDQUIST, K. (2010). Functional groups and bonding patterns in lignin. In C. Heitner, D. Dimmel, & J. Schmidt (Eds.), *Lignins and lignans – advances in chemistry* (pp. 267–301). Boca Raton, FL: Taylor & Francis Group, LCC.

CALVO-FLORES, F., DOBADO, J., ISAC-GARCIA, J., & MARTIN-MARTINEZ, F. (2015). *Lignin and lignans as renewable raw materials – Chemistry, technology and applications*. Singapore: John Wiley & Sons, LTD.

CATALKAYA, E. C., & KARGI, F. (2007). Color, TOC and AOX removals from pulp mill effluent by advanced oxidation processes: A comparative study. *Journal of Hazardous Materials*, *139*(2), 244–253. https://doi.org/10.1016/j.jhazmat.2006.06.023

CHANG, H., & ALLAN, G. (1971). Oxidation. In K. Sarkanen & C. Ludwig (Eds.), *Lignins – Occurrence, formation, structure and reactions* (pp. 433–487). New York: John Wiley & Sons, LTD.

DANG, B. T. T., BRELID, H., & THELIANDER, H. (2016). The impact of ionic strength on the molecular weight distribution (MWD) of lignin dissolved during softwood kraft

cooking in a flow-through reactor. *Holzforschung*, *70*(6), 495–501. https://doi.org/10.1515/hf-2015-0103

DE LOS SANTOS RAMOS, W., POZNYAK, T., CHAIREZ, I., & CÓRDOVA R., I. (2009). Remediation of lignin and its derivatives from pulp and paper industry wastewater by the combination of chemical precipitation and ozonation. *Journal of Hazardous Materials*, *169*(1–3), 428–434. https://doi.org/10.1016/j.jhazmat.2009.03.152

DIMMEL, D. (2010). Overview. In C. Heitner, D. Dimmel, & J. Schmidt (Eds.), *Lignins and lignans – advances in chemistry* (pp. 1–11). Boca Raton, FL: Taylor & Francis Group, LCC.

DIMMEL, D., & GELLERSTEDT, G. (2010). Chemistry of alkaline pulping. In C. Heitner, D. Dimmel, & J. Schmidt (Eds.), *Lignins and lignans – advances in chemistry* (pp. 349–393). Boca Raton, FL: Taylor & Francis Group, LCC.

FENGEL, D., & WEGENER, G. (1983). *Wood. Chemistry, ultrastructure, reactions*. Berlin, GER: Walter de Gruyter, GmbH & Co KG.

FONTANIER, V., BAIG, S., ALBET, J., & MOLINIER, J. (2005). Comparison of Conventional and Catalytic Ozonation for the Treatment of Pulp Mill Wastewater. *Environmental Engineering Science*, *22*(2), 127–137. https://doi.org/10.1089/ees.2005.22.127

FONTANIER, V., FARINES, V., ALBET, J., BAIG, S., & MOLINIER, J. (2006). Study of catalyzed ozonation for advanced treatment of pulp and paper mill effluents. *Water Research*, *40*(2), 303–310. https://doi.org/10.1016/j.watres.2005.11.007

GELLERSTEDT, G. (2009a). Chemistry of Bleaching of Chemical Pulp. In M. Ek, G. Gellerstedt, & G. Henriksson (Eds.), *Pulp and paper chemistry and technology Vol. 2* (pp. 201–239). Berlin, GER: Walter de Gruyter, GmbH & Co KG.

GELLERSTEDT, G. (2009b). Chemistry of chemical pulping. In M. Ek, G. Gellerstedt, & G. Henriksson (Eds.), *Pulp and paper chemistry and technology Vol. 2* (pp. 91–121). Berlin, GER: Walter de Gruyter, GmbH & Co KG.

GELLERSTEDT, G. (2010). Chemistry of pulp bleaching. In C. Heitner, D. Dimmel, & J. Schmidt (Eds.), *Lignins and lignans – advances in chemistry* (pp. 393–439). Boca Raton, FL: Taylor & Francis Group, LCC.

GERMGARD, U. (2009a). Bleaching of Pulp. In M. Ek, G. Gellerstedt, & G. Henriksson (Eds.), *Pulp and paper chemistry and technology Vol. 2* (pp. 239–277). Berlin, GER: Walter de Gruyter, GmbH & Co KG.

GERMGARD, U. (2009b). Production of Bleaching Chemicals at the Mill. In G. Gellerstedt, G. Henriksson, & M. Ek (Eds.), *Pulp and paper chemistry and technology Vol. 2* (pp. 277–297). Berlin, GER: Walter de Gruyter, GmbH & Co KG.

GOGATE, P. R., & PANDIT, A. B. (2004). A review of imperative technologies for wastewater treatment I: Oxidation technologies at ambient conditions. *Advances in Environmental Research*, *8*(3–4), 501–551. https://doi.org/10.1016/S1093-0191(03)00032-7

GOLDSCHMID, O. (1971). Ultraviolet spectra. In K. Sarkanen & C. Ludwig (Eds.), *Lignins – Occurrence, formation, structure and reactions* (pp. 241–267). New York: John Wiley & Sons, LTD.

GREENBERG, A. E. (1992). Standard methods for the examination of water and wastewater. Washington, D.C: American Public Health Assoc.

HEITNER, C., DIMMEL, D., & SCHMIDT, J. (2010). *Lignins and lignans – advances in chemistry*. Boca Raton, FL: Taylor & Francis Group, LCC.

HOIGNÉ, J., & BADER, H. (1983a). Rate constants of reactions of ozone with organic and inorganic compounds in water-I. Non-dissociating organic compounds. *Water Research*. https://doi.org/10.1016/0043-1354(83)90098-2

HOIGNÉ, J., & BADER, H. (1983b). Rate constants of reactions of ozone with organic and inorganic compounds in water-II. Dissociating organic compounds. *Water Research*. https://doi.org/10.1016/0043-1354(83)90099-4

HORVÁTH, M., BILITZKY, L., & HÜTTNER, J. (1985). *Ozone*. (R. Clark, Ed.), *Topics in inorganic and general chemistry. Vol. 20*. Amsterdam: Elsevier Science Publishers.

HÜBSCHMANN, H. (2001). *Handbook of GC/MS – Fundamentals and applications*. Weinheim: Wiley-VCH Verlag.

KALLIOLA, A., ASIKAINEN, M., TALJA, R., & TAMMINEN, T. (2014). Experiences of kraft lignin functionalization by enzymatic and chemical oxidation. *BioResources*, *9*(4), 7336–7351.

KALLIOLA, KUITUNEN, S., LIITIÄ, T., ROVIO, S., OHRA-AHO, T., VUORINEN, T., & TAMMINEN, T. (2011). Lignin oxidation mechanisms under oxygen delignification conditions. Part 1. Results from direct analyses. *Holzforschung*. https://doi.org/10.1515/hf.2011.101

KALLIOLA, VEHMAS, T., LIITIÄ, T., & TAMMINEN, T. (2015). Alkali-O2 oxidized lignin - A bio-based concrete plasticizer. *Industrial Crops and Products*, *74*, 150–157. https://doi.org/10.1016/j.indcrop.2015.04.056

KARAT, I. (2013). Advanced Oxidation Processes for Removal of COD from Pulp and Paper Mill Effluents. *Diva-Portal.Org*. Retrieved from http://www.diva-portal.org/smash/get/diva2:618554/FULLTEXT02.pdf

KO, C. H., HSIEH, P. H., CHANG, M. W., CHERN, J. M., CHIANG, S. M., & TZENG, C. J. (2009). Kinetics of pulp mill effluent treatment by ozone-based processes. *Journal of Hazardous Materials*, *168*(2–3), 875–881. https://doi.org/10.1016/j.jhazmat.2009.02.111

KREETACHAT, T., DAMRONGSRI, M., PUNSUWON, V., VAITHANOMSAT, P., CHIEMCHAISRI, C., & CHOMSURIN, C. (2007). Effects of ozonation process on lignin-derived compounds in pulp and paper mill effluents. *Journal of Hazardous Materials*, *142*(1–2), 250–257. https://doi.org/10.1016/j.jhazmat.2006.08.011

KUITUNEN, S., KALLIOLA, A., TARVO, V., TAMMINEN, T., ROVIO, S., LIITIÄ, T., … ALOPAEUS, V. (2011). Lignin oxidation mechanisms under oxygen delignification conditions. Part 3. Reaction pathways and modeling. *Holzforschung*. https://doi.org/10.1515/hf.2011.100

LAI, Y., & SARKANEN, K. (1971). Isolation and structural studies. In K. Sarkanen & C. Ludwig (Eds.), *Lignins – Occurrence, formation, structure and reactions* (pp. 165–

241). New York: John Wiley & Sons, LTD.

LANGLAIS, B., RECKHOW, D., & BRINK, D. (1991). *Ozone in water treatment – Application and engineering.* Chelsea, MI: Lewis Publishers, Inc.

LEARY, G., & SCHMIDT, J. (2010). Chemistry of lignin-retaining bleaching: Oxidative bleaching agents. In C. Heitner, D. Dimmel, & J. Schmidt (Eds.), *Lignins and lignans – advances in chemistry* (pp. 439–471). Boca Raton, FL: Taylor & Francis Group, LCC.

LEI, L., & LI, Y. (2014). Effect of Ozonation on Recalcitrant Chemical Oxygen Demand (COD), Color, and Biodegradability of Hardwood Kraft Pulp (KP) Bleaching Effluent. *BioResources*, *9*(1), 1236–1245.

LIFTINGER, E., ZWECKMAIR, T., SCHILD, G., EILENBERGER, G., BÖHMDORFER, S., ROSENAU, T., & POTTHAST, A. (2015). Analysis of degradation products in rayon spinning baths. *Holzforschung*, *69*(6), 695–702. https://doi.org/10.1515/hf-2014-0278

MARTON, J. (1971). Reactions in alkaline pulping. In K. Sarkanen & C. Ludwig (Eds.), *Lignins – Occurrence, formation, structure and reactions* (pp. 639–695). New York: John Wiley & Sons, LTD.

MERAYO, N., HERMOSILLA, D., BLANCO, L., CORTIJO, L., & BLANCO, Á. (2013). Assessing the application of advanced oxidation processes, and their combination with biological treatment, to effluents from pulp and paper industry. *Journal of Hazardous Materials*, *262*, 420–427. https://doi.org/10.1016/j.jhazmat.2013.09.005

RALPH, J., LUNDQUIST, K., BRUNOW, G., LU, F., KIM, H., SCHATZ, P. F., … BOERJAN, W. (2004). Lignins: Natural polymers from oxidative coupling of 4-hydroxyphenyl-propanoids. *Phytochemistry Reviews*, *3*(1), 29–60. https://doi.org/10.1023/B:PHYT.0000047809.65444.a4

RICE, R. (1986). Applications of ozone in water and wastewater treatment. In R. Rice, J. Bollyky, & W. Lacy (Eds.), *Analytical aspects of ozone treatment of water and wastewater*. Chelsea, MI: Lewis Publishers, Inc.

RINALDI, R., JASTRZEBSKI, R., CLOUGH, M. T., RALPH, J., KENNEMA, M., BRUIJNINCX, P. C. A., & WECKHUYSEN, B. M. (2016). Paving the Way for Lignin Valorisation: Recent Advances in Bioengineering, Biorefining and Catalysis. *Angewandte Chemie - International Edition*, *55*(29), 8164–8215. https://doi.org/10.1002/anie.201510351

ROVIO, S., KUITUNEN, S., OHRA-AHO, T., ALAKURTTI, S., KALLIOLA, A., & TAMMINEN, T. (2011). Lignin oxidation mechanisms under oxygen delignification conditions. Part 2: Advanced methods for the detailed characterization of lignin oxidation mechanisms. *Holzforschung*. https://doi.org/10.1515/hf.2011.088

SARKANEN, K., & HERGERT, H. (1971). Classification and distribution. In K. Sarkanen & C. Ludwig (Eds.), *Lignins – Occurrence, formation, structure and reactions* (pp. 43–95). New York: John Wiley & Sons, LTD.

SARKANEN, K., & LUDWIG, C. (1971a). Definiton and Nomenclature. In K. Sarkanen & C. Ludwig (Eds.), *Lignins – Occurrence, formation, structure and reactions* (pp. 1–19). New York: John Wiley & Sons, LTD.

SARKANEN, K., & LUDWIG, C. (1971b). *Lignins – Occurrence, formation, structure and reactions*. New York: John Wiley & Sons, LTD.

SCHMIDT, J. (2010). Electronic Spectroscopy of Lignins. In C. Heitner, D. Dimmel, & J. Schmidt (Eds.), *Lignins and lignans – advances in chemistry* (pp. 49–103). Boca Raton, FL: Taylor & Francis Group, LCC.

SCHWEDT, G. (2008). *Analytische Chemie – Grundlagen, Methoden und Praxis* (Second). Weinheim: Wiley-VCH Verlag.

SIXTA, H. (2006). *Handbook of pulp*. Weinheim: Wiley-VCH Verlag.

SUMERSKII, I., KORNTNER, P., ZINOVYEV, G., ROSENAU, T., & POTTHAST, A. (2015). Fast track for quantitative isolation of lignosulfonates from spent sulfite liquors. *RSC Advances*, *5*(112), 92732–92742. https://doi.org/10.1039/C5RA14080C

SUZUKI, H., CAO, J., JIN, F., KISHITA, A., ENOMOTO, H., & MORIYA, T. (2006). Wet oxidation of lignin model compounds and acetic acid production. *Journal of Materials Science*, *41*(5), 1591–1597. https://doi.org/10.1007/s10853-006-4653-9

WANG, R., CHEN, C. L., & GRATZL, J. S. (2004). Ozonation of pine kraft lignin in alkaline solution. Part 1: Ozonation, characterization of kraft lignin and its ozonated preparations. *Holzforschung*, *58*(6), 622–630. https://doi.org/10.1515/HF.2004.116

YEBER, M. C., RODRÍGUEZ, J., FREER, J., BAEZA, J., DURÁN, N., & MANSILLA, H. D. (1999). Advanced oxidation of a pulp mill bleaching wastewater. *Chemosphere*, *39*(10), 1679–1688. https://doi.org/10.1016/S0045-6535(99)00068-5

ZAKZESKI, J., BRUIJNINCX, P. C. A., JONGERIUS, A. L., & WECKHUYSEN, B. M. (2010). The Catalytic Valorization of Ligning for the Production of Renewable Chemicals. *Chem. Rev.*, *110*, 3552–3599. https://doi.org/10.1021/cr900354u

ZHU, W., & THELIANDER, H. (2015). Precipitation of lignin from softwood black liquor: An investigation of the equilibrium and molecular properties of lignin. *BioResources*, *10*(1), 1696–1714.

ZHU, W., WESTMAN, G., & THELIANDER, H. (2014). Investigation and Characterization of Lignin Precipitation in the LignoBoost Process. *Journal of Wood Chemistry and Technology*, *34*(2), 77–97. https://doi.org/10.1080/02773813.2013.838267